ORGANOMETALLICS

Article

pubs.acs.org/Organometallics

"Backdoor Induction" of Chirality: Asymmetric Hydrogenation with Rhodium(I) Complexes of Triphenylphosphane-Substituted β-Turn Mimetics

Zoran Kokan, Zoran Glasovac, Maja Majerić Elenkov, Matija Gredičak, Ivanka Jerić, and Srećko I. Kirin*

Ruđer Bošković Institute, Bijenička cesta 54, HR-10000 Zagreb, Croatia

Supporting Information

ABSTRACT: Bioconjugate bidentate ligands **2**–**10** were obtained by tethering triphenylphosphanecarboxylic acid to amino acid substituted spacers with different flexibility, ranging from a rigid enediyne-based β-turn inducer to flexible linear aliphatic chains with up to eight carbon atoms. The 21 synthesized ligands revealed up to 81% ee selectivity in rhodium-catalyzed asymmetric hydrogenation of α,β-unsaturated amino acids. The key feature of the catalysts is the prochiral coordination sphere of the catalytic metal while the chirality is transmitted by "backdoor induction" from distant hydrogen-bonded amino acids. DFT calculations were applied to study the structure and relative stability of the precatalytic organometallic Rh(I) complexes, with particular emphasis on hydrogen-bonded secondary structures.

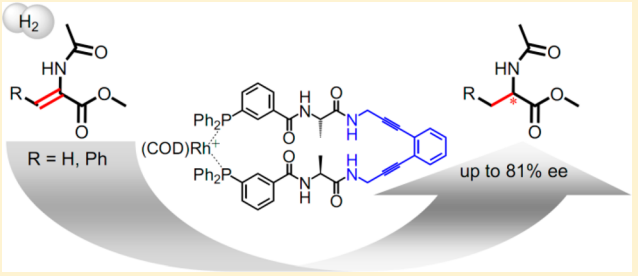

INTRODUCTION

β-Turns are among three main secondary structural motifs found in peptides and proteins.[1] Mimetics with turnlike structures are involved in various interactions between biomolecules;[2] therefore, new scaffolds able to act as β-turn initiators are highly desirable. Generally, turnlike structures are known to be stabilized by the presence of conformational constraints, additional hydrogen bond donating and accepting groups, or peptide bond trans−cis isomerization.[3−5]

A rather general model which may be used for efficient β-turn template screening is based on geometric analysis of the distances between C_α atoms in various β-turn fragments.[6] A cluster analysis of tetraalanyl peptide segments, constructed by using torsion angles of different idealized β-turn types, identified clear patterns with a triangle relationship (Chart 1a). We have reported that templates based on amino acids bridged with a rigid *cis*-enediyne moiety have predefined turnlike conformation while maintaining enough flexibility to adjust upon addition of metal ions.[7] Moreover, the close resemblance with one class of β-turn geometry was found when applying geometric analysis on C_α surrogates in our templates (Chart 1b).

Recently, we have used triphenylphosphane amino acid bioconjugates as bioinspired monodentate ligands in Rh(I)-catalyzed asymmetric hydrogenation of α,β-unsaturated amino acids.[8−12] Those $[Rh(COD)(\mathbf{Lig})_2]BF_4$ complexes feature a prochiral catalytically active metal; the chirality is transmitted by "backdoor induction" from distant hydrogen-bonded amino acids (Chart 2).[8,13] Herein, we tether monodentate ligands to rigid or flexible linkers that allow different spatial arrangements of hydrogen bond donor and acceptor groups (of the amino acids) and as a consequence different phosphane−rhodium−

Chart 1. Triangle Relationship of (a) C_α atoms (Solid Squares) in a Near-Isosceles Pattern Found in β-Turns[5] and (b) C_α Surrogates (Open Squares) in Peptide Mimetics Described Herein, Calculated for the Bis-*N*-Acetyl Derivative using B3LYP/6-31G(d)[a]

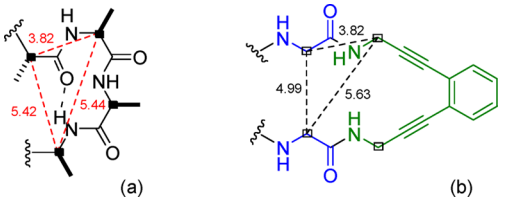

[a]Distances are given in Å.

Chart 2. Side View (Left) and Top View (Right) of Meta-Substituted $[Rh(COD)(Lig)_2]BF_4$ Complexes[a]

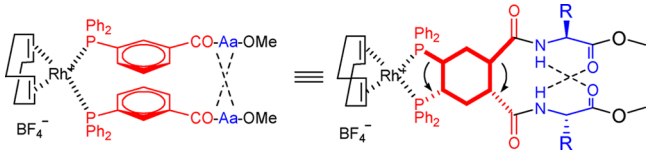

[a]The upper central aromatic ring is indicated in boldface; the arrows indicate the sign of helical chirality.

Received: May 19, 2014
Published: July 30, 2014

   dx.doi.org/10.1021/om5005385 | *Organometallics* 2014, 33, 4005−4015

phosphane bite angles[14] and study the influence of the various linkers on the selectivity in asymmetric hydrogenation.

RESULTS AND DISCUSSION

Synthesis and Characterization. Monodentate ligand amino acid bioconjugates **1A** and **1A$_p$** were prepared by standard peptide coupling in solution (TBTU/HOBt/DIPEA), reacting Boc-Ala-OH with meta- or para-substituted (diphenylphosphane)benzoic acid **I** or **II**, respectively (Scheme 1).[15]

Scheme 1. [a]

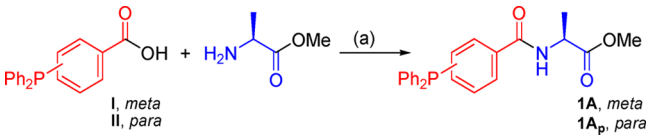

[a]Reagents and conditions: (a) Boc-Ala-OMe, TBTU/HOBt/DIPEA, DCM, room temperature, 15 h.

Bidentate ligand bioconjugates **2A**–**8A**, **4AA**, and **5AA** were synthesized according to Scheme 2. First, the *N*-Boc-protected derivatives **Boc-2A**–**Boc-8A**, **Boc-4AA**, and **Boc-5AA** were prepared using 2 equiv of Boc-Ala-OH and 1 equiv of diamines NH_2-$(CH_2)_n$-NH_2 with different chain lengths, n = 2–8. In the second step, the Boc derivatives were deprotected under standard conditions (TFA/DCM) and further coupled with meta-substituted triphenylphosphanecarboxylic acid **II** via the TBTU/HOBt/DIPEA protocol to give ligand amino acid or dipeptide bioconjugates **2A**–**8A**, **4AA**, and **5AA**.

The synthesis of bidentate ligand bioconjugates **9** and **10** is highlighted in Scheme 3. Sonogashira coupling of alanine, leucine, valine, or phenylalanine *N*-propargyl amides[16] and 1,2-diiodobenzene was performed in THF in the presence of piperidine, $Pd(PPh_3)_4$, and CuI to yield Boc-enediynes **Boc-9**. Catalytic hydrogenation of **Boc-9** using Pd/C in MeOH gave Boc derivatives **Boc-10**. Ligand bioconjugates **9** and **10** were obtained by *N*-terminal deprotection of **Boc-9** and **Boc-10** (TFA/DCM), followed by coupling with triphenylphosphanes **I** or **II** under standard conditions (TBTU/HOBt/DIPEA).

Asymmetric Hydrogenation. Organometallic precatalyst complexes [Rh(COD)**Lig**]BF_4 with bidentate ligands, **Lig** = **2**–**10**, prepared in situ were used in asymmetric hydrogenation of α,β-unsaturated amino acids **S1** and **S2** (Scheme 4). Their catalytic activity was compared to that of in situ prepared complexes [Rh(COD)(**Lig**)$_2$]BF_4 with monodentate ligands, **Lig** = **1A**, **1A$_p$**; the results are collected in Tables 1 and 2.

All examined Rh complexes proved to be efficient hydrogenation catalysts with excellent conversion of the substrate to the product. Thus, optimal conditions for hydrogenation of **S1** are 2 h at room temperature and ambient pressure, while optimal conditions for **S2** are 2 h at room temperature and elevated H_2 pressure (13 bar).

In particular, rigid enediyne ligands **9** generally show higher selectivity than supramolecular ligand **1** or derivatives **10** with a more flexible linker. The best result with up to 81% ee was obtained using the meta-substituted alanine ligand **9A** with a small side chain (Table 1, run 6). Catalysis with previously reported diphenylphosphane–isophthalic acid based ligands also gave the highest selectivity if alanine derivatives were used.[8a]

A significant difference in selectivity was obtained for meta- and para-substituted ligands. Meta-substituted ligands **9** and **10** revealed moderate to good selectivity, mostly above 50% ee for both substrates. In contrast, for all para-substituted ligands **1A$_p$**, **9A$_p$**, **9L$_p$**, **10A$_p$**, and **10L$_p$**, the selectivity in catalysis was generally below 20% ee (see Table S1, Supporting Information). The favorable displaced stacking of the central aromatic rings in meta-substituted ligands (see (i) in Chart 3) can be used to explain the significantly higher selectivity in catalysis, as opposed to the less favorable face-to-face stacked

Scheme 2. [a]

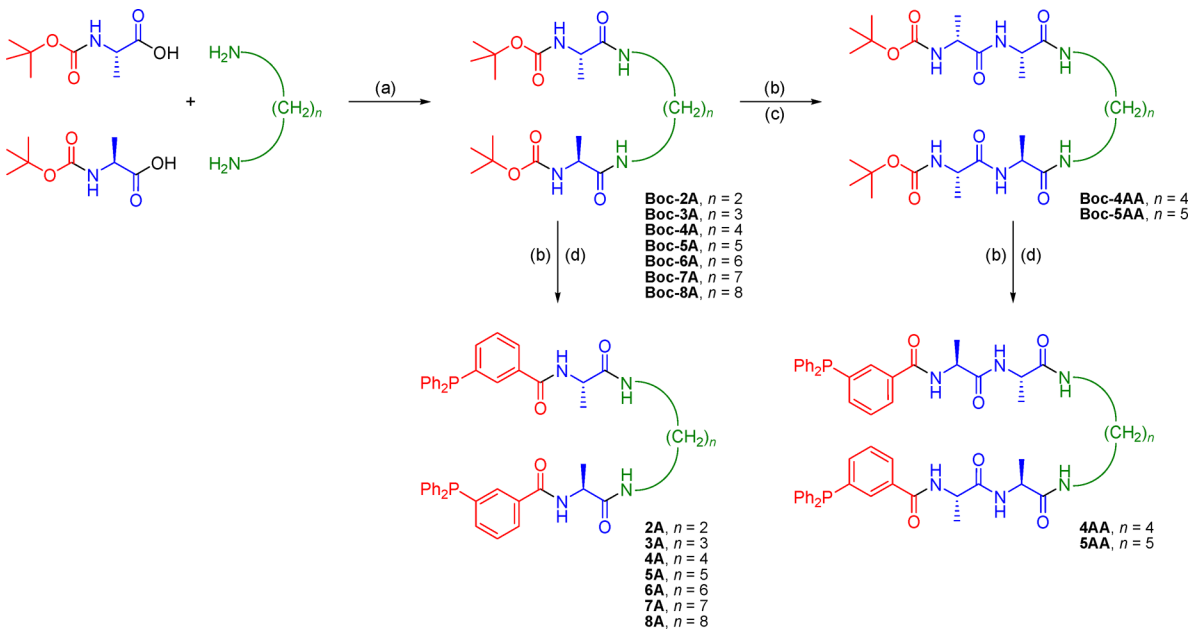

[a]Reagents and conditions: (a) TBTU/HOBt/DIPEA, DCM, room temperature, 15 h; (b) TFA/DCM (1/1); (c) Boc-Ala-OMe, TBTU/HOBt/DIPEA, DCM, room temperature, 15 h; (d) Ph_2P-*m*C_6H_4-CO_2H/TBTU/HOBt/DIPEA, DCM, room temperature, 15 h.

dx.doi.org/10.1021/om5005385 | *Organometallics* 2014, 33, 4005–4015

Scheme 3. [a]

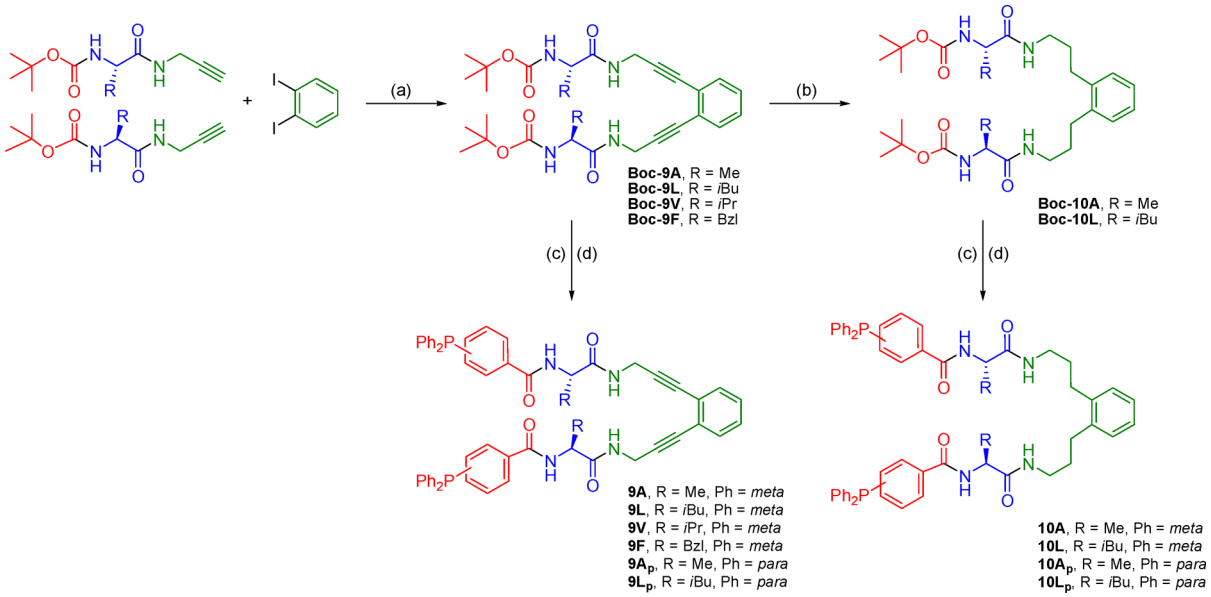

[a]Reagents and conditions: (a) piperidine (2 equiv), $Pd(PPh_3)_4$ (0.01 equiv), CuI (0.1 equiv)/THF; (b) Pd/C/MeOH; (c) TFA/DCM (1/1); (d) Ph_2P-C_6H_4-CO_2H/TBTU/HOBt/DIPEA, DCM, room temperature, 15 h.

Scheme 4. [a]

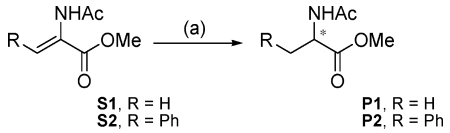

[a]Reagents and conditions: (a) [Rh(COD)**Lig**]BF_4/H_2/DCM (0.1 M substrate), room temperature; [Rh]/**Lig**/substrate = 1/1.1/100.

Table 1. Rh(I)-Catalyzed Asymmetric Hydrogenation of S1 or S2 by using Meta-Substituted Ligands 1, 9, and 10[a]

run	ligand	substrate	t (h)	p (bar)	conversn (%)[b]	ee (R) (%)[c]
1	**1A**/**1A**	**S1**	2	1	>98	56 (S)/3 (S)[e]
2	**1A**/**1A**	**S2**	20	1	47	58 (S)
3	**1A**/**1A**	**S2**	2	13	>98	61 (S)
4	**9A**	**S1**	2	1	>98	75/56[e]
5	**9A**	**S1**	2	1	>98	73[d]
6	**9A**	**S2**	20	1	89	81
7	**9A**	**S2**	2	13	90	53
8	**9V**	**S1**	2	1	>98	58
9	**9V**	**S2**	20	1	63	63
10	**9V**	**S2**	2	13	81	35
11	**9L**	**S1**	2	1	>98	61
12	**9L**	**S2**	20	1	78	70
13	**9L**	**S2**	2	13	>98	49
14	**9F**	**S1**	2	1	>98	53
15	**9F**	**S2**	20	1	63	61
16	**9F**	**S2**	2	13	87	40
17	**10A**	**S1**	2	1	>98	44
18	**10A**	**S2**	20	1	>98	60
19	**10A**	**S2**	2	13	>98	16
20	**10L**	**S1**	2	1	>98	45
21	**10L**	**S2**	20	1	>98	36
22	**10L**	**S2**	2	13	>98	7

[a]Reaction according to Scheme 4. [b]Determined by ^{1}H NMR spectroscopic analysis. [c]Determined by GC analysis: BetaDex 225 for **S1**/**P1** and L-Chirasil-Val for **S2**/**P2**. [d]Reaction performed at −5 °C. [e]MeOH was used as solvent.

aromatic rings in the para-substituted ligands ((ii) in Chart 3).[17]

The opposite stereochemical outcome of the catalytic reaction was obtained for meta-substituted bidentate ligands **9** and **10**, in comparison to monodentate ligand **1A** (Table 1). Using monodentate ligand **1A**, the catalysis resulted in up to 61% ee in favor of (*S*)-**P1** or (*S*)-**P2**; this result is in agreement with our previous stereochemical analysis.[8b,13] However, if meta-substituted bidentate ligands **9** and **10** are used, an excess of (*R*)-**P1** or (*R*)-**P2** is obtained in catalytic hydrogenation.

Next, in an attempt to investigate the importance of structural rigidity in catalysis, instead of the rigid enediyne (in ligands **9**), aliphatic chains with varying length (up to eight carbon atoms) were incorporated in bidentate phosphane ligands **2A**−**8A**. Meta substitution of the ligand and amino acid building block alanine were retained, because meta-substituted alanine ligands were the most selective catalysts so far. In the **2A**−**8A** series of ligands, the highest selectivity in the studied asymmetric hydrogenation was 72% ee (*R*) for the optimal spacer length of n = 5 (Table 2, entry 10). Adding one amino acid per chain in **4AA** and **5AA** did not improve the selectivity (Table 2, entries 22−27). Interestingly, for a series of ligands **8A**, **10A**, and **9A**, all with an eight-carbon-atom spacer, the selectivity significantly increases upon constraining the spacer by means of a phenyl ring and/or triple bonds (Chart 4), indicating that complexes with rigid spacers give more structurally defined intermediates in the catalytic cycle.

At ambient pressure, the selectivity of the catalysts for both **S1** and **S2** is mostly similar, often with slightly higher ee values in the asymmetric hydrogenation of **S2**. Catalysis under increased hydrogen pressure resulted in a significant decrease of selectivity for **S2** using bidentate meta ligands **9** and **10**, while it had almost no effect on para ligands (Table S1,

dx.doi.org/10.1021/om5005385 | *Organometallics* 2014, 33, 4005−4015

Chart 3. Different Stacking of the Central Aromatic Rings: (i) Meta- and (ii) Para-Substitution Pattern[a]

[a]The lower ring is indicated with a dashed line.

Table 2. Rh(I)-Catalyzed Asymmetric Hydrogenation of S1 or S2 by using Ligands 2–8[a]

run	ligand	substrate	t (h)	p (bar)	conversn (%)[b]	ee (R) (%)[c]
1	**2A**	**S1**	2	1	>98	8
2	**2A**	**S2**	20	1	92	1
3	**2A**	**S2**	2	13	>98	4
4	**3A**	**S1**	2	1	>98	22
5	**3A**	**S2**	20	1	>98	8
6	**3A**	**S2**	2	13	>98	24
7	**4A**	**S1**	2	1	>98	51/8[d]
8	**4A**	**S2**	20	1	>98	47
9	**4A**	**S2**	2	13	>98	19
10	**5A**	**S1**	2	1	>98	65
11	**5A**	**S2**	20	1	>98	72
12	**5A**	**S2**	2	13	>98	39
13	**6A**	**S1**	2	1	>98	16
14	**6A**	**S2**	20	1	>98	22
15	**6A**	**S2**	2	13	>98	12 (S)
16	**7A**	**S1**	2	1	>98	48
17	**7A**	**S2**	20	1	>98	55
18	**7A**	**S2**	2	13	>98	6
19	**8A**	**S1**	2	1	>98	13 (S)
20	**8A**	**S2**	20	1	>98	9 (S)
21	**8A**	**S2**	2	13	>98	23 (S)
22	**4AA**	**S1**	2	1	>98	29 (S)
23	**4AA**	**S2**	20	1	>98	22 (S)
24	**4AA**	**S2**	2	13	>98	12 (S)
25	**5AA**	**S1**	2	1	>98	39
26	**5AA**	**S2**	20	1	>98	48
27	**5AA**	**S2**	2	13	>98	23

[a]Reaction according to Scheme 4. [b]Determined by ^{1}H NMR spectroscopic analysis. [c]Determined by GC analysis: BetaDex 225 for **S1**/**P1** and L-Chirasil-Val for **S2**/**P2**. [d]MeOH was used as solvent.

Chart 4. Spacers Incorporated in Ligands 8A, 10A, and 9A in Comparison to the Selectivity Obtained in Catalysis of S1 (Upper Row) or S2 (Lower Row)[a]

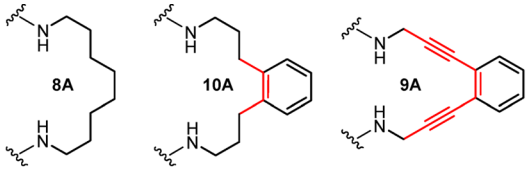

[a]Constrained carbon atoms are highlighted in red.

Supporting Information). Monodentate ligand **1A** (Table 1, entries 2 and 3) exhibited only a slight change in selectivity for **S2** at higher pressure, which is in accordance with our previous work.[8a] Ligands with an alkyl spacer reveal an increase of selectivity with **3A** and **8A** (Table 2, entries 5, 6 and 20, 21), and an inversion of selectivity with **6A** (Table 2, entries 14, 15).

When the solvent is changed from dichloromethane to methanol (Tables 1 and 2), the quantitative yield of the catalytic hydrogenation is retained, while the selectivity decreases. In the case of ligands **1A** and **4A**, the selectivity is completely lost: 56% to 3% ee (Table 1, entry 1) and 51% to 8% ee (Table 2, entry 8), respectively. However, if **9A** is used as ligand in Rh(I)-catalyzed hydrogenation, moderate selectivity is retained (Table 1, entry 4, 75% to 56% ee). These results reveal the importance of hydrogen bonds for inducing selectivity, as shown in our previous work.[8a]

Precatalyst Rh(I) Complexes. *Spectroscopy.* Rh(I) complexes with ligands **1**–**10**, with 2:1 phosphorus donor to metal stoichiometry, were prepared in situ and studied by NMR and CD spectroscopy. The absence of amide proton resonances below δ 7 ppm in ^{1}H NMR spectra of Rh(I) complexes in a non-hydrogen-bonding solvent ($CDCl_3$) indicates the involvement of amide protons in hydrogen bonding, suggesting an ordered structure of the metal complexes in solution (see the Supporting Information). CD spectra of the Rh(I) complexes further support an ordered structure in CH_2Cl_2 solution (Chart 5). In particular, CD signals of the Rh chromophore strongly support efficient "backdoor induction" of chirality from the chiral amino acids to the prochiral rhodium.[8,18−20]

Chart 5. CD Spectra of Selected Organometallic Precatalytic Complexes [Rh(COD)(Lig)]BF_4 in CH_2Cl_2

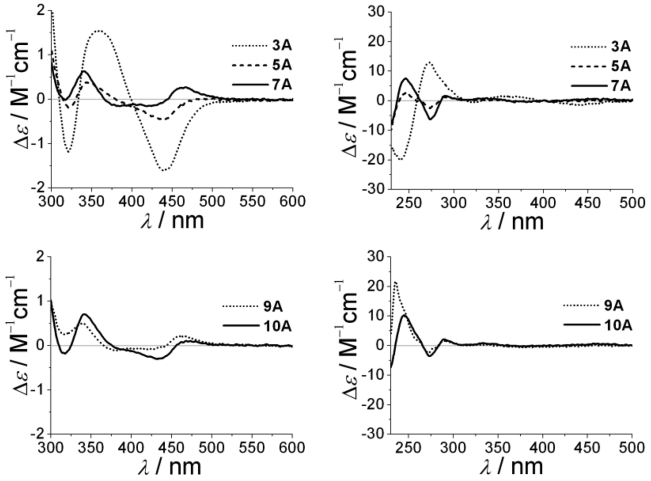

Computational Study. Relative energies of Rh(I) precatalyst complexes were calculated using two theoretical methods. First, the widely accepted general purpose B3LYP approach was employed (**M1** method), which has been used earlier for investigation of the gas-phase chemistry of metal complexes.[21] The second calculation method, **M2**, using the M06-L density functional is parametrized against a training set containing noncovalent interactions including $\pi-\pi$ interactions and was recommended for calculation of metal complexes.[22]

In our study, supramolecular complexes with monodentate ligands [Rh(COD)(**1Lig**)$_2$]$^+$ as well as complexes with bidentate ligands [Rh(COD)(**9Lig**)]$^+$ were calculated; amino acid substituents were achiral glycine or chiral L-alanine. Geometry optimization of all investigated structures led to a square-planar rhodium coordination, as found in X-ray crystal structures of [Rh(COD)(PPh_3)$_2$]$^+$ derivatives.[23] Since the tetrafluoroborate anion does not coordinate to the metal,

dx.doi.org/10.1021/om5005385 | Organometallics 2014, 33, 4005−4015

only the cations were calculated; the anion was left out for simplicity.

For each metal complex, several conformers based on different hydrogen-bonding patterns between the two parallel amino acid strands were considered (Chart 6). The conformers

Chart 6. Different Hydrogen Bonding Patterns: Conformers a, b, c1, and c2 Exemplified at the Amino Acid Substituted Enediyne Backbone[a]

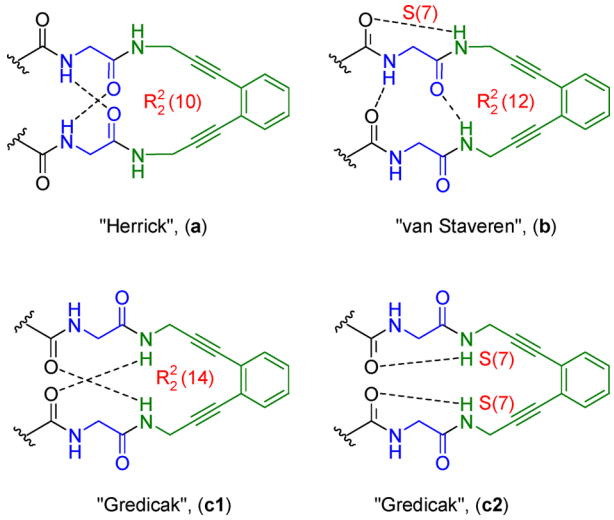

[a]Hydrogen bonds are indicated by dashed lines; Bernstein–Davis notation is indicated in red, according to ref 24.

can be distinguished by looking at the carbonyl oxygen atoms directly attached to the triphenylphosphane moiety: the "Herrick conformer" **a** features both carbonyl oxygen atoms directly attached to the triphenylphosphane moiety pointing away from the cleft formed by the two amino acids. In the "van Staveren conformer" **b**, one carbonyl oxygen atom points toward the cleft and the other carbonyl oxygen points away, while in the "Gredičak conformer" **c** both carbonyl oxygen atoms point inward. If the Bernstein–Davis classification is applied,[24] the conformers differ in the number of atoms involved in the hydrogen-bonded rings: $R_2^2(10)$ for **a**, $R_2^2(12)$ for **b**, $R_2^2(14)$ for **c1** with interstrand hydrogen bonds, and an additional hydrogen bond with S(7) notation is possible in conformer **b**. On the other hand, conformer **c2** contains two S(7) intrastrand hydrogen bonds.

The relative energies of the various conformers are collected in Table 3. Slightly different results with the two theoretical methods could be expected; our calculations show, however, that both methods predict the same trend of stabilities for the studied conformers.

For the "Herrick conformer" two different substitution patterns of $\pi-\pi$ stacked meta-disubstituted phenyl rings were considered: stretched conformer **a1** and crowded conformer **a2** (Chart 7). It is important to note that the same helical chirality of the hydrogen-bonded amino acid substituents, for example *P* in Chart 7, induces opposite chirality at the metal coordination sphere, *M* for **a1** and *P* for **a2**. For the "van Staveren conformer" **b**, geometrical optimization surprisingly predicts $\pi-\pi$ stacking between one meta-disubstituted phenyl ring and one monosubstituted phenyl ring. "Gredičak conformer" **c1** with interstrand hydrogen bonds was not identified as a minimum on the potential energy surface (PES). During

Table 3. Relative Energies (E_{rel}) of Several Conformers of the Achiral (Lig = G) and Chiral (Lig = A) Precatalytic Complexes Calculated Using Theoretical Models M1 and M2[a]

			E_{rel}/kJ mol^{-1}		
				Lig = A	
	conformer		Lig = G	*M*-1,2′[b]	*P*-1,2′[b]
[Rh(COD)(**1Lig**)$_2$]$^+$	**a1**	**M1**	0.0	0.0	17.3
		(**M2**)	(0.0)	(0.0)	(5.4)
	a2	**M1**	8.4	28.0	12.3
		(**M2**)	(9.6)	(12.2)	(12.4)
	b	**M1**	25.0	30.6	37.9
		(**M2**)	(41.9)	(44.4)	(44.9)
[Rh(COD)(**9Lig**)]$^+$	**a1**	**M1**	0.0	0.0	30.9
		(**M2**)	(0.0)	(0.0)	(28.8)
	a2	**M1**	6.6	30.4	6.2
		(**M2**)	(4.7)	(25.5)	(13.1)
	b	**M1**	10.8	8.5	43.1
		(**M2**)	(28.2)	(26.3)	(46.9)

[a]Relative energies (E_{rel}) were calculated by either the B3LYP (**M1** model) or M06-L (**M2** model) density functional method at the same optimized geometries. The most stable conformation was used as the reference structure. [b]Configuration of the Rh metallacycle; see Chart 7 for an explanation.

Chart 7. Different Substitution Patterns a1 and a2 of the Meta-Disubstituted Rings in the Rh(I) Complexes[25,a]

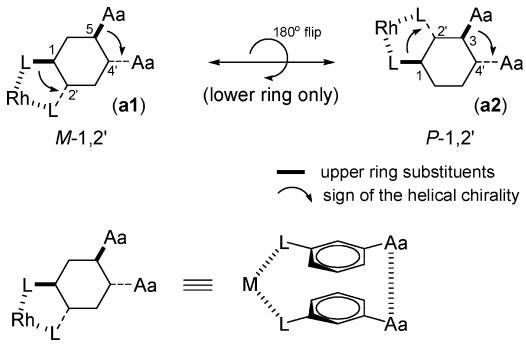

[a]For a detailed stereochemical analysis see the Supporting Information.

optimization, interstrand hydrogen bonds cleaved and intrastrand hydrogen bonds were established, ending up in the **c2** conformer that is, however, 50 kJ mol^{-1} above the most stable conformer **a1**. Additional attempts to optimize the **c1** conformer starting from **c1**-like initial geometries were not successful. Therefore, only conformers **a** and **b** were studied in detail, while the least stable conformer **c2** was abandoned.

The achiral supramolecular complex [Rh(COD)(**1G**)$_2$]$^+$ was studied first (Table 3). In this case, the conformers differ in the number of hydrogen bonds: conformers **a1** and **a2** each contain two hydrogen bonds, while conformer **b** has one such bond. Both applied theoretical models **M1** and **M2** predicted "Herrick conformer" **a1** to be the most stable (Table 3). The highest stability of "Herrick conformer" **a** is expected, since this conformer is found in the single crystal of [Pt(**1VA**)$_2$Cl$_2$],[9d] and **a** is also present in the ferrocene peptides.[13,26] However, while **a1** is significantly more stable than **b** (ΔE_{rel} > 25 kJ mol^{-1}), the relative energies of the crowded conformer **a2** are

dx.doi.org/10.1021/om5005385 | *Organometallics* 2014, 33, 4005–4015

rather close to those of **a1** (ΔE_{rel} = 6.6 (**M1**) and 4.7 kJ mol^{-1} (**M2**)) (Table 3).

Next, the achiral macrocyclic complex [Rh(COD)(**9G**)]$^+$ was calculated. Including the β-turn mimicking building block introduces two more amide protons capable of hydrogen bonding. Again, the conformers differ in the number of hydrogen bonds: conformers **a1** and **a2** contain two hydrogen bonds each, and conformer **b** has three H bonds. The results obtained reveal that "Herrick conformer" **a1** is the most stable for [Rh(COD)(**9G**)]$^+$ as well, followed by **a2** and **b**, but the energy difference between **a1** and **b** is only 10.8 kJ mol^{-1} (by **M2**) (Table 3).

Complexes [Rh(COD)(**1A**)$_2$]$^+$ and [Rh(COD)(**9A**)]$^+$ containing the chiral amino acid alanine have also been calculated. In these chiral derivatives, interstrand hydrogen bonding between the two amino acids induces helical chirality at the stacked phenyl rings, leading to different stereoisomers (Table 3). The trends found for achiral glycine derivatives apply also for chiral alanine analogues: (i) "Herrick conformers" **a** are more stable than the "van Staveren" conformers **b** and (ii) the difference between **a** and **b** is larger for the supramolecular complex [Rh(COD)(**1A**)$_2$]$^+$ than for the bidentate complex [Rh(COD)(**9A**)]$^+$. However, only small energetic differences were calculated for conformers with different helical chiralities of the rhodium coordination sphere that would lead to opposite configurations of the product in catalysis. For the chiral supramolecular complex [Rh(COD)(**1A**)$_2$]$^+$ ΔE_{rel} between 1,2′-*M* **a1** and 1,2′-*P* **a1** is only 5.4 kJ mol^{-1} (by the **M2** theoretical model). In addition, for chiral bidentate complex [Rh(COD)(**9A**)]$^+$, three conformers of different helical chiralities are found to be within 10 kJ mol^{-1}: 1,2′-*P* **a2** and 1,2′-*M* **b** are only 6.2 and 8.5 kJ mol^{-1} (using **M1** theoretical model) less stable than 1,2′-*M* **a1**. From the small energy differences calculated for the studied conformers of precatalytic complexes, it is not possible to predict a general trend for the configuration of the preferred product in catalysis.

CONCLUSION

Bidentate triphenylphosphane amino acid ligands **Lig** containing β-turn inducing linkers with different flexibilities have been synthesized and characterized. Precatalytic organometallic rhodium(I) complexes [Rh(COD)(**Lig**)]BF$_4$ adopt an ordered structure in non-hydrogen-bonding solvents, as shown by NMR and CD spectroscopy. The structure and relative stability of selected precatalytic complexes was studied by DFT calculations using the two theoretical models B3LYP and M06-L and showed that stretched "Herrick conformer" **a1** is the most stable, but the difference in stability from that of the crowded "Herrick conformer" **a2** can be rather small: ΔE_{rel} < 10 kJ mol^{-1}.

The rhodium complexes were used as catalysts in asymmetric hydrogenation of α,β-unsubstituted amino acids. Bidentate ligands described in this study yielded more selective catalysts than their monodentate analogues (61% ee (*S*) with monodentate ligand **1A**). The nature of the linker in the bidentate ligands has a major influence on the selectivity in catalysis. In particular, enantioselectivities up to 81% ee (*R*) were obtained with ligand **9A**, containing the most favorable rigid enediyne linker. Within the series of ligands with different lengths of the flexible −NH(CH$_2$)$_n$NH− linker, the best result was obtained with ligand **5A**: *n* = 5, 72% ee (*R*). The presented catalysts are enzyme models where an artificial chiral β-turn serves as a minimal but functional outer coordination sphere that controls the chirality of the prochiral catalytic metal in asymmetric catalysis. The results obtained herein clearly show that the chiral information far away from the catalytic metal has a significant impact on enantioselectivity in the studied hydrogenation reaction.

It is important to point out that subtle changes to the architecture of our L-amino acid substituted ligands allow access to both enantiomers of the catalytic product: while monodentate ligand **1A** yields an excess of the *S* product, introducing a linker in the most selective bidentate ligands **9A** and **5A** results in predominant formation of the *R* product. In order to explain this turnover in selectivity and predict the configuration of the major product in catalysis, detailed experimental and computational data on the reaction mechanism are necessary.[12] Work along these lines is in progress in our laboratories.

EXPERIMENTAL SECTION

General Methods. Reactions were carried out in ordinary glassware, and chemicals were used as purchased from commercial suppliers without further purification. Pure L-amino acids were used. Reactions were monitored by TLC on silica gel 60 F254 plates and detected with a UV lamp (254 nm) or ninhydrin; compounds were purified using automated flash chromatography equipped with a UV detector (254 nm) and prepacked silica columns. For reactions at low temperature, a cryostat device was used.

Mass spectra were measured on a HPLC-MS system coupled with 6410 triple-quadrupole mass spectrometer, operating in a positive ESI mode. High-resolution mass spectra were obtained on a MALDI TOF-TOF instrument using a CHCA matrix. CD spectra were recorded on a spectropolarimeter in 1 cm quartz Suprasil cells. NMR spectra were obtained on spectrometers operating at 300.13 or 600.13 MHz for ^{1}H, 75.47 or 150.92 MHz for ^{13}C, and 242.93 MHz for ^{31}P nuclei. Chemical shifts, δ (ppm), indicate a downfield shift from the internal standard tetramethylsilane (TMS) for ^{1}H NMR, H_3PO_4 (85%) for ^{31}P NMR, or residual solvent signal for ^{13}C NMR (77.16 ppm for $CDCl_3$ or 39.52 ppm for DMSO-d_6). Coupling constants, *J*, are given in Hz. Enantiomeric excesses were determined on a gas chromatograph (FID detector) using chiral fused silica capillary columns Beta Dex 225 (30 m × 0.25 mm × 0.25 μm) or Permabond L-Chirasil-Val (25 m × 0.25 mm).

Computational Details. All calculations were performed using the Gaussian09 program package.[28] Geometries were optimized using the B3LYP hybrid density functional[29] in conjunction with the Ahlrichs SVP basis set[30] for the first-row elements and TZVP basis set for phosphorus, while the LanL2DZ effective core potential[31] was employed for rhodium. Electronic energies were recalculated using two different density functionals, indicated throughout the text as the calculation models **M1** and **M2**. The first model (**M1**) encompasses a B3LYP hybrid density functional in conjunction with LanL2DZ ECP for rhodium and TZVP basis set for other elements. Alternatively, model **M2** was constructed by choosing the M06-L density functional,[22] in combination with Pople's 6-311++G(3df,2p) (C, H, O, N, and P) and LanL2DZ (Rh) basis sets. The nature of the stationary points was verified by vibrational analysis at the optimized geometries, and no imaginary frequencies were obtained. Total energies (E_{tot}) were obtained by summing **M1** or **M2** electronic energies with zero-point vibrational energies (E_{ZPV}) without any scaling of the latter. Visualization of the optimized structures was done by MOLDEN 5.0.[32]

Ligands. *Peptide Coupling: General Procedure.* 5-(Diphenylphosphino)isophthalic acid, TBTU, HOBt, and DIPEA were stirred at room temperature in DCM. After 1 h, amino acid or peptide was added to the reaction mixture and stirring was continued overnight (approximately 15 h). The reaction mixture was then washed with $NaHCO_3$ (saturated aqueous), citric acid (10%, aqueous), and NaCl (saturated aqueous), dried over Na_2SO_4, filtered,

dx.doi.org/10.1021/om5005385 | Organometallics 2014, 33, 4005−4015

evaporated under vacuum, and purified by automated flash chromatography on a prepacked silica column.

Boc Protecting Group Removal. The corresponding Boc-protected amino acid or peptide was dissolved in DCM/trifluoroacetic acid (1/1, 5 mL) and the solution stirred for 2 h at room temperature. The volatiles were evaporated under reduced pressure, and the viscous residue was dissolved in 15 mL of DCM. The residual trifluoroacetic acid was neutralized with excess DIPEA (0.5 mL). This solution was used for further peptide synthesis.

1A. 3-(Diphenylphosphino)benzoic acid (126.9 mg, 0.41 mmol), HOBt (53.39 mg, 0.40 mmol), TBTU (132.1 mg, 0.41 mmol), DIPEA (0.140 mL, 0.85 mmol), H-Ala-OMe·HCl (61.7 mg, 0.44 mmol), DCM (50 mL). Chromatography on silica (12 g), EtOAc/hexane gradient (TLC: R_f = 0.60, EtOAc/hexane 1/1). Yield: 109.1 mg (67%). ^{1}H NMR (600,14 MHz, $CDCl_3$) δ/ppm: 1.48 (d, 3H, J = 7 Hz), 3.77 (s, 3H), 4.73−4.77 (m, 1H), 6.59 (d, 1H, J = 7 Hz), 7.29−7.42 (m, 12H), 7.76−7.78 (m, 2H). ^{13}C NMR ($CDCl_3$, 75.48 MHz) δ/ppm: 18.7 (β), 48.7 (α), 52.7 (OMe), 127.7 (4), 128.8 (d, $^3J_{CP}$ = 7 Hz, 3′, 3″), 128.9 (d, $^3J_{CP}$ = 6 Hz, 5), 129.2 (4′, 4″), 132.3 (d, $^2J_{CP}$ = 25 Hz, 2), 133.9 (d, $^2J_{CP}$ = 20 Hz, 2′, 2″), 134.3 (d, $^3J_{CP}$ = 8 Hz, 3), 136.6, 136.6 (d, $^1J_{CP}$ = 11 Hz, 1′, 1″), 136.8 (d, $^2J_{CP}$ = 15 Hz, 6), 138.7 (d, $^1J_{CP}$ = 13 Hz, 1), 166.6 (7), 173.7 (A1). ESI-MS (m/z): 392.2 (M + H$^+$, 100%). MALDI-HRMS (m/z): calcd 392.1410 ($C_{23}H_{22}NO_3P$ + H$^+$), found 392.1402.

1A$_p$. 4-(Diphenylphosphino)benzoic acid (117.8 mg, 0.39 mmol), HOBt (43.1 mg, 0.32 mmol), TBTU (97.1 mg, 0.30 mmol), DIPEA (0.200 mL, 1.21 mmol), H-Ala-OMe·HCl (48.5 mg, 0.35 mmol), DCM (50 mL). Chromatography on silica (12 g), EtOAc/hexane gradient (TLC: R_f = 0.46, EtOAc/hexane 1/1). Yield: 84.1 mg (71%). ^{1}H NMR (600,14 MHz, $CDCl_3$) δ/ppm: 1.51 (d, 3H, J = 7 Hz), 3.79 (s, 3H), 4.77−4.82 (m, 1H), 6.69 (d, 1H, J = 7 Hz), 7.29−7.37 (m, 12H), 7.74 (dd, 2H, J_1 = 8 Hz, J_2 = 1 Hz). ^{13}C NMR ($CDCl_3$, 150.92 MHz) δ/ppm: 18.8 (β), 48.7 (α), 52.7 (OMe), 127.1 (d, $^3J_{CP}$ = 6.5 Hz, 3, 6), 128.8 (d, $^3J_{CP}$ = 7 Hz, 3′, 3″), 129.2 (4′, 4″), 133.7 (d, $^2J_{CP}$ = 19 Hz, 2, 6), 134.0 (d, $^2J_{CP}$ = 20 Hz, 3, 5), 134.1 (4), 136.5 (d, $^1J_{CP}$ = 11 Hz, 1′, 1″), 142.7 (d, $^1J_{CP}$ = 14 Hz, 1), 166.6 (7), 173.7 (A1). ^{31}P NMR ($CDCl_3$, 242.93 MHz) δ/ppm: −5.08. ESI-MS (m/z): 430.4 (M + K$^+$, 53%). MALDI-HRMS (m/z): calcd 392.1410 ($C_{23}H_{22}NO_3P$ + H$^+$), found 392.1415.

2A. 3-(Diphenylphosphino)benzoic acid (133.2 mg, 0.43 mmol), HOBt (61.7 mg, 0.46 mmol), TBTU (134.5 mg, 0.42 mmol), DIPEA (0.145 mL, 0.88 mmol), **Boc-2A** (84.9 mg, 0.21 mmol), DCM (50 mL). Chromatography (DCM/MeOH gradient; TLC, R_f = 0.20, DCM/MeOH 10/0.5). Yield: 76.7 mg (45%). ^{1}H NMR ($CDCl_3$, 300.13 MHz) δ/ppm: 1.40 (d, 6H, J = 7 Hz), 3.20−3.30 (m, 2H), 3.42−3.54 (m, 2H), 4.48−4.57 (m, 2H), 6.82 (d, 2H, J = 7 Hz), 6.92 (t, 2H, J = 4 Hz), 7.24−7.35 (m, 22H), 7.69 (dt, 2H, J_1 = 7.5 Hz, J_2 = 1.5 Hz), 7.79 (dt, 2H, J_1 = 8 Hz, J2 = 1.5 Hz). ^{13}C NMR ($CDCl_3$, 150.92 MHz) δ/ppm: 18.3 (β), 39.6 (a), 49.9 (α), 127.6 (4), 128.8 (d, $^3J_{CP}$ = 7 Hz, 3′, 3″), 128.9 (d, $^3J_{CP}$ = 5.5 Hz, 5), 129.2 (4′, 4″), 132.7 (d, $^2J_{CP}$ = 25 Hz, 2), 133.9 (d, $^2J_{CP}$ = 19 Hz, 2′), 133.9 (d, $^2J_{CP}$ = 19 Hz, 2″), 134.0 (d, $^3J_{CP}$ = 8 Hz, 3), 136.6 (d, $^1J_{CP}$ = 11 Hz, 1′), 136.6 (d, $^1J_{CP}$ = 11 Hz, 1″), 136.8 (d, $^2J_{CP}$ = 14.5 Hz, 6), 138.8 (d, $^1J_{CP}$ = 13.5 Hz, 1), 167.3 (7), 173.5 (A1). ESI-MS (m/z): 801.3 (M + Na$^+$, 100%). MALDI-HRMS (m/z): calcd 779.2910 ($C_{46}H_{44}N_4O_4P_2$ + H$^+$), found 779.2906.

3A. 3-(Diphenylphosphino)benzoic acid (137.1 mg, 0.45 mmol), HOBt (63.4 mg, 0.47 mmol), TBTU (141.3 mg, 0.44 mmol), DIPEA (0.145 mL, 0.88 mmol), **Boc-3A** (92.8 mg, 0.22 mmol), DCM (50 mL). Chromatography (DCM/MeOH gradient; TLC, R_f = 0.20, DCM/MeOH 9.5/0.5). Yield: 107.9 mg (61%). ^{1}H NMR ($CDCl_3$, 600.14 MHz) δ/ppm: 1.42 (d, 6H, J = 7 Hz), 1.64−1.68 (m, 2H), 3.09−3.14 (m, 2H), 3.42−3.47 (m, 2H), 4.58−4.63 (m, 2H), 6.78 (d, 2H, J = 7 Hz), 7.10 (t, 2H, J = 6 Hz), 7.27−7.35 (m, 22H), 7.74 (dt, 2H, J_1 = 7 Hz, J_2 = 1.5 Hz), 7.80 (dt, 2H, J_1 = 8 Hz, J2 = 1.5 Hz). ^{13}C NMR ($CDCl_3$, 150.92 MHz) δ/ppm: 18.4 (β), 29.0 (b), 37.1 (a), 49.8 (α), 127.6 (4), 128.8 (d, $^3J_{CP}$ = 7 Hz, 3′, 3″), 128.9 (d, $^3J_{CP}$ = 6 Hz, 5), 129.2 (4′, 4″), 132.7 (d, $^2J_{CP}$ = 26 Hz, 2), 133.9 (d, $^2J_{CP}$ = 20 Hz, 2′), 133.9 (d, $^2J_{CP}$ = 19 Hz, 2″), 134.1 (d, $^3J_{CP}$ = 8 Hz, 3), 136.6 (d, $^1J_{CP}$ = 11 Hz, 1′, 1″), 136.8 (d, $^2J_{CP}$ = 14 Hz, 6), 138.7 (d, $^1J_{CP}$ = 13.5 Hz, 1), 167.3 (7), 173.0 (A1). ESI-MS (m/z): 793.3 (M + H$^+$, 100%). MALDI-HRMS (m/z): calcd 793.3067 ($C_{47}H_{46}N_4O_4P_2$ + H$^+$), found 793.3071.

4A. 3-(Diphenylphosphino)benzoic acid (132.3 mg, 0.43 mmol), HOBt (62.8 mg, 0.46 mmol), TBTU (135.1 mg, 0.42 mmol), DIPEA (0.145 mL, 0.88 mmol), **Boc-4A** (92.8 mg, 0.22 mmol), DCM (50 mL). Chromatography (DCM/MeOH gradient; TLC, R_f = 0.18, DCM/MeOH 10/0.5). Yield: 93.6 mg (54%). ^{1}H NMR ($CDCl_3$, 300.13 MHz) δ/ppm: 1.29−1.42 (m, 4H), 1.43 (d, 6H, J = 7 Hz), 2.92−3.03 (m, 2H), 3.22−3.33 (m, 2H), 4.69−4.78 (m, 2H), 7.04 (d, 2H, J = 8 Hz), 7.08 (dd, 2H, J_1 = 6 Hz, J_2 = 5 Hz), 7.24−7.36 (m, 22H), 7.70 (dt, 2H, J_1 = 7.5 Hz, J_2 = 1.5 Hz), 7.79 (dt, 2H, J_1 = 8 Hz, J_2 = 1.5 Hz). ^{13}C NMR ($CDCl_3$, 150.92 MHz) δ/ppm: 18.8 (β), 26.4 (b), 39.2 (a), 49.5 (α), 127.4 (4), 128.8 (d, $^3J_{CP}$ = 7 Hz, 3′, 3″), 128.8 (d, $^3J_{CP}$ = 6 Hz, 5), 129.1, 129.1 (4′, 4″), 132.8 (d, $^2J_{CP}$ = 24.5 Hz, 2), 133.9 (d, $^2J_{CP}$ = 19 Hz, 2′), 133.9 (d, $^2J_{CP}$ = 20.5 Hz, 2″), 134.0 (d, $^3J_{CP}$ = 6 Hz, 3), 136.5 (d, $^1J_{CP}$ = 11 Hz, 1′), 136.6 (d, $^1J_{CP}$ = 10.5 Hz, 1″), 136.8 (d, $^2J_{CP}$ = 15 Hz, 6), 138.7 (d, $^1J_{CP}$ = 14 Hz, 1), 167.3 (7), 173.0 (A1). ^{31}P NMR ($CDCl_3$, 242.93 MHz) δ/ppm: −5.09. ESI-MS (m/z): 829.4 (M + Na$^+$, 43%). MALDI-HRMS (m/z): calcd 807.3223 ($C_{48}H_{48}N_4O_4P_2$ + H$^+$), found 807.3227.

4AA. 3-(Diphenylphosphino)benzoic acid (104.7 mg, 0.34 mmol), HOBt (48.0 mg, 0.36 mmol), TBTU (105.6 mg, 0.33 mmol), DIPEA (0.150 mL, 0.91 mmol), **Boc-4AA** (91.1 mg, 0.16 mmol), DCM (50 mL). Chromatography (DCM/MeOH gradient; TLC, R_f = 0.26, DCM/MeOH 9.5/0.5). Yield: 112.4 mg (69%). ^{1}H NMR (DMSO-d_6, 600.14 MHz) δ/ppm: 1.18 (d, 6H, J = 7 Hz), 1.31 (d, 6H, J = 7 Hz), 1.33−1.35 (m, 4H), 2.93−2.99 (m, 2H), 3.01−3.06 (m, 2H), 4.18−4.23 (m, 2H), 4.39−4.43 (m, 2H), 7.24−7.27 (m, 8H) 7.29−7.32 (m, 2H), 7.39−7.42 (m, 12H), 7.48−7.50 (m, 2H), 7.70 (t, 2H, J = 5.5 Hz), 7.88−7.93 (m, 6H), 8.57 (d, 2H, J = 7 Hz). ^{13}C NMR ($CDCl_3$, 150.92 MHz) δ/ppm: 17.6, 18.3 (1,2β), 26.2 (b), 38.1 (a), 48.1, 49.2 (1,2α), 128.0 (4), 128.6 (d, $^3J_{CP}$ = 5 Hz, 5), 128.8 (d, $^3J_{CP}$ = 7 Hz, 3′, 3″), 129.0, 129.1 (4′, 4″), 132.7 (d, $^2J_{CP}$ = 26 Hz, 2), 133.2 (d, $^2J_{CP}$ = 20 Hz, 2′), 133.2 (d, $^2J_{CP}$ = 19.5 Hz, 2″), 134.2 (d, $^3J_{CP}$ = 8 Hz, 3), 135.6 (d, $^2J_{CP}$ = 14 Hz), 136.2 (d, $^1J_{CP}$ = 11 Hz, 1′), 136.2 (d, $^1J_{CP}$ = 11.5 Hz, 1″), 137.1 (d, $^1J_{CP}$ = 13 Hz, 1), 165.8 (7), 171.8 (1,2A1). ESI-MS (m/z): 949.4 (M + H$^+$, 100%). MALDI-HRMS (m/z): calcd 949.3965 ($C_{54}H_{58}N_6O_6P_2$ + H$^+$), found 949.3981.

5A. 3-(Diphenylphosphino)benzoic acid (126.6 mg, 0.41 mmol), HOBt (60.0 mg, 0.44 mmol), TBTU (131.2 mg, 0.41 mmol), DIPEA (0.145 mL, 0.88 mmol), **Boc-5A** (94.6 mg, 0.21 mmol), DCM (50 mL). Chromatography (DCM/MeOH gradient; TLC, R_f = 0.21, DCM/MeOH 9.5/0.5). Yield: 66.0 mg (39%). ^{1}H NMR ($CDCl_3$, 600.14 MHz) δ/ppm: 1.16−1.21 (m, 2H), 1.40−1.49 (m, 4H), 1.45 (d, 6H, J = 7 Hz), 2.98−3.02 (m, 2H), 3.32−3.37 (m, 2H), 4.71−4.76 (m, 2H), 6.92 (dd, 2H, J_1 = 6.5 Hz, J_2 = 4 Hz), 7.21−7.33 (m, 24H), 7.69 (dt, 2H, J_1 = 8 Hz, J_2 = 1.5 Hz), 7.81 (dt, 2H, J_1 = 8 Hz, J_2 = 1.5 Hz). ^{13}C NMR ($CDCl_3$, 75.48 MHz) δ/ppm: 18.2 (β), 23.0 (c), 28.2 (b), 38.8 (a), 49.3 (α), 127.4 (4), 128.8 (d, $^3J_{CP}$ = 7 Hz, 3′, 3″), 128.9 (d, $^3J_{CP}$ = 8 Hz, 5), 129.1 (4′, 4″), 133.0 (d, $^2J_{CP}$ = 26 Hz, 2), 133.9 (d, $^2J_{CP}$ = 20 Hz, 2′, 2″), 134.0 (d, $^3J_{CP}$ = 8 Hz, 3), 136.6 (d, $^1J_{CP}$ = 11 Hz, 1′, 1″), 136.8 (d, $^2J_{CP}$ = 14 Hz, 6), 138.6 (d, $^1J_{CP}$ = 13.5 Hz, 1), 167.4 (7), 173.1 (A1). ^{31}P NMR ($CDCl_3$, 242.93 MHz) δ/ppm: −5.07. ESI-MS (m/z): 821.3 (M + H$^+$, 43%). MALDI-HRMS (m/z): calcd 821.3380 ($C_{49}H_{50}N_4O_4P_2$ + H$^+$), found 821.3361.

5AA. 3-(Diphenylphosphino)benzoic acid (93.9 mg, 0.31 mmol), HOBt (47.6 mg, 0.35 mmol), TBTU (101.6 mg, 0.32 mmol), DIPEA (0.150 mL, 0.91 mmol), **Boc-5AA** (93.3 mg, 0.16 mmol), DCM (50 mL). Chromatography (DCM/MeOH gradient; TLC, R_f = 0.27, DCM/MeOH 9.5/0.5). Yield: 92.8 mg (63%). ^{1}H NMR (DMSO-d_6, 600.14 MHz) δ/ppm: 1.17−1.22 (m, 2H), 1.18 (d, 6H, J = 7 Hz), 1.31 (d, 6H, J = 7 Hz), 1.32−1.37 (m, 4H), 2.93−3.04 (m, 4H), 4.18−4.23 (m, 2H), 4.38−4.43 (m, 2H), 7.24−7.27 (m, 8H) 7.29−7.32 (m, 2H), 7.39−7.42 (m, 12H), 7.48−7.51 (m, 2H), 7.66 (t, 2H, J = 5.5 Hz), 7.89−7.93 (m, 6H), 8.58 (d, 2H, J = 7 Hz). ^{13}C NMR ($CDCl_3$, 75.48 MHz) δ/ppm: 17.6, 18.2 (1,2β), 23.5 (c), 28.6 (b), 38.4 (a), 48.1, 49.3 (1,2α), 128.0 (4), 128.6 (d, $^3J_{CP}$ = 5 Hz, 5), 128.8 (d, $^3J_{CP}$ = 7 Hz, 3′, 3″), 129.1 (4′, 4″), 132.7 (d, $^2J_{CP}$ = 26 Hz, 2), 133.2 (d, $^2J_{CP}$ = 19.5 Hz, 2′), 133.3 (d, $^2J_{CP}$ = 19.5 Hz, 2″), 134.2 (d, $^3J_{CP}$ = 8 Hz, 3), 135.7

dx.doi.org/10.1021/om5005385 | *Organometallics* 2014, 33, 4005−4015

(d, $^2J_{CP}$ = 14 Hz), 136.2 (d, $^1J_{CP}$ = 11 Hz, 1′), 136.2 (d, $^1J_{CP}$ = 11 Hz, 1″), 137.1 (d, $^1J_{CP}$ = 13 Hz, 1), 165.8 (7), 171.7, 171.8 (1,2A1). ESI-MS (*m*/*z*): 963.4 (M + H$^+$, 100%). MALDI-HRMS (*m*/*z*): calcd 963.4122 ($C_{55}H_{60}N_6O_6P_2$ + H$^+$), found 963.4124.

6A. 3-(Diphenylphosphino)benzoic acid (148.0 mg, 0.48 mmol), HOBt (67.0 mg, 0.50 mmol), TBTU (154.0 mg, 0.48 mmol), DIPEA (0.160 mL, 0.97 mmol), **Boc-6A** (116.1 mg, 0.25 mmol), DCM (50 mL). Chromatography (DCM/MeOH gradient; TLC, R_f = 0.24, DCM/MeOH 10/0.5). Yield: 111.01 mg (55%). ^{1}H NMR ($CDCl_3$, 300.13 MHz) δ/ppm: 1.11−1.28 (m, 4H), 1.33−1.41 (m, 4H), 1.44 (d, 6H, *J* = 7 Hz), 2.92−3.03 (m, 2H), 3.18−3.29 (m, 2H), 4.65−4.75 (m, 2H), 6.82 (t, 2H, *J* = 5.5 Hz), 7.21 (d, 2H, *J* = 8 Hz), 7.24−7.34 (m, 22H), 7.74 (dt, 2H, J_1 = 7 Hz, J_2 = 1.5 Hz), 7.82 (dt, 2H, J_1 = 8 Hz, J_2 = 1 Hz). ^{13}C NMR ($CDCl_3$, 75.48 MHz) δ/ppm: 18.3 (β), 25.4 (c), 28.8 (b), 38.7 (a), 49.4 (α), 127.5 (4), 128.8 (d, $^3J_{CP}$ = 7 Hz, 3′, 3″), 128.8 (d, $^3J_{CP}$ = 4 Hz, 5), 129.1 (4′, 4″), 132.9 (d, $^2J_{CP}$ = 24.5 Hz, 2), 133.8 (d, $^2J_{CP}$ = 19.5 Hz, 2′, 2″), 134.1 (d, $^3J_{CP}$ = 6.5 Hz, 3), 136.6 (d, $^1J_{CP}$ = 11 Hz, 1′, 1″), 136.8 (d, $^2J_{CP}$ = 14 Hz, 6), 138.6 (d, $^1J_{CP}$ = 13 Hz, 1), 167.2 (7), 172.7 (A1). ESI-MS (*m*/*z*): 835.4 (M + H$^+$, 100%). MALDI-HRMS (*m*/*z*): calcd 835.3536 ($C_{50}H_{52}N_4O_4P_2$ + H$^+$), found 835.3558.

7A. 3-(Diphenylphosphino)benzoic acid (123.6 mg, 0.40 mmol), HOBt (55.5 mg, 0.41 mmol), TBTU (124.8 mg, 0.39 mmol), DIPEA (0.145 mL, 0.88 mmol), **Boc-7A** (94.9 mg, 0.20 mmol), DCM (50 mL). Chromatography (DCM/MeOH gradient; TLC, R_f = 0.27, DCM/MeOH 9.5/0.5). Yield: 84.4 mg (49%). ^{1}H NMR ($CDCl_3$, 600.14 MHz) δ/ppm: 1.13 (s, 1H), 1.24−1.30 (m, 2H), 1.46 (d, 6H, *J* = 7 Hz), 2.87−2.92 (m, 2H), 3.23−3.28 (m, 2H), 4.75−4.80 (m, 2H), 6.96 (t, 2H, *J* = 5.5 Hz), 7.26−7.34 (m, 24H), 7.77 (dt, 2H, J_1 = 7.5 Hz, J_2 = 1.5 Hz), 7.85 (dt, 2H, J_1 = 8 Hz, J2 = 1.5 Hz). ^{13}C NMR ($CDCl_3$, 105.92 MHz) δ/ppm: 18.4 (β), 25.7 (c), 27.7 (d), 28.3 (b), 39.3 (a), 49.2 (α), 127.6 (4), 128.7 (5, overlapped with 3′ peak), 128.8 (d, $^3J_{CP}$ = 7 Hz, 3′, 3″), 129.1 (4′, 4″), 133.1 (d, $^2J_{CP}$ = 26 Hz, 2), 133.9 (d, $^2J_{CP}$ = 20 Hz, 2′), 133.9 (d, $^2J_{CP}$ = 19 Hz, 2″), 134.1 (d, $^3J_{CP}$ = 8 Hz, 3), 136.6 (d, $^1J_{CP}$ = 11 Hz, 1′, 1″), 136.8 (d, $^2J_{CP}$ = 14.5 Hz, 6), 138.5 (d, $^1J_{CP}$ = 13 Hz, 1), 167.2 (7), 172.8 (A1). ESI-MS (*m*/*z*): 849.4 (M + H$^+$, 100%). MALDI-HRMS (*m*/*z*): calcd 849.3693 ($C_{51}H_{54}N_4O_4P_2$ + H$^+$), found 849.3696.

8A. 3-(Diphenylphosphino)benzoic acid (148.2 mg, 0.48 mmol), HOBt (71.0 mg, 0.53 mmol), TBTU (156.7 mg, 0.49 mmol), DIPEA (0.160 mL, 0.97 mmol), **Boc-8A** (107.4 mg, 0.22 mmol), DCM (50 mL). Chromatography (DCM/MeOH gradient; TLC, R_f = 0.15, EtOAc/hexane 7/3). Yield: 124.09 mg (59%). ^{1}H NMR ($CDCl_3$, 300.13 MHz) δ/ppm: 1.14 (s, 8H), 1.29−1.37 (m, 4H), 1.44 (d, 6H, *J* = 7 Hz), 2.91−3.03 (m, 2H), 3.23−3.34 (m, 2H), 4.66−4.76 (m, 2H), 6.81 (t, 2H, *J* = 5.5 Hz), 7.07 (d, 2H, *J* = 8 Hz), 7.25−7.36 (m, 22H), 7.73−7.77 (m, 2H), 7.81 (d, 2H, *J* = 8 Hz). ^{13}C NMR ($CDCl_3$, 75.48 MHz) δ/ppm: 18.6 (β), 25.9 (c), 28.4 (d), 29.1 (b), 39.4 (a), 49.4 (α), 127.5 (4), 128.8 (d, $^3J_{CP}$ = 7 Hz, 3′, 3″), 128.8 (d, $^3J_{CP}$ = 5 Hz, 5), 129.1 (4′, 4″), 132.8 (d, $^2J_{CP}$ = 24.5 Hz, 2), 133.9 (d, $^2J_{CP}$ = 19.5 Hz, 2′, 2″), 134.1 (d, $^3J_{CP}$ = 8 Hz, 3), 136.5 (d, $^1J_{CP}$ = 11 Hz, 1′, 1″), 136.7 (d, $^2J_{CP}$ = 14 Hz, 6), 138.6 (d, $^1J_{CP}$ = 13.5 Hz, 1), 167.1 (7), 172.5 (A1). ESI-MS (*m*/*z*): 885.3 (M + Na$^+$, 14%). MALDI-HRMS (*m*/*z*): calcd 863.3849 ($C_{52}H_{56}N_4O_4P_2$ + H$^+$), found 863.3835.

9A. 3-(Diphenylphosphino)benzoic acid (76.7 mg, 0.25 mmol), HOBt (39.2 mg, 0.29 mmol), TBTU (81.3 mg, 0.25 mmol), DIPEA (0.165 mL, 1.00 mmol), **Boc-9A** (60.2 mg, 0.11 mmol), DCM (50 mL). Chromatography (EtOAc/hexane gradient; TLC, R_f = 0.49, EtOAc/hexane 7/3). Yield: 33.6 mg (33%). ^{1}H NMR ($CDCl_3$, 300.14 MHz) δ/ppm: 1.49 (d, 6H, *J* = 7 Hz), 4.02 (dd, 2H, J_1 = 17.5 Hz, J_2 = 4.5 Hz), 4.30 (dd, 2H, J_1 = 17.5 Hz, J_2 = 6 Hz), 4.83−4.93 (m, 2H), 7.19−7.38 (m, 28H), 7.65 (pseudo-t, 2H, *J* = 5 Hz), 7.75 (dt, 2H, J_1 = 7.5 Hz, J_2 = 1 Hz), 7.86 (d, 2H, J_1 = 7.5 Hz, J_2 = 1 Hz). ^{13}C NMR ($CDCl_3$, 150.92 MHz) δ/ppm: 18.2 (β), 30.3 (a), 49.3 (α), 81.6 (b), 88.9 (c), 125.9 (d), 127.6 (4), 128.1 (f), 128.8 (d, $^3J_{CP}$ = 7 Hz, 3′, 3″), 128.8 (5, under the 3′ peak), 129.1 (4′, 4″), 131.7 (e), 133.1 (d, $^2J_{CP}$ = 26 Hz, 2), 133.9 (d, $^2J_{CP}$ = 19 Hz, 2′), 133.9 (d, $^2J_{CP}$ = 19 Hz, 2″), 133.9 (d, $^3J_{CP}$ = 6 Hz, 3), 136.6 (d, $^1J_{CP}$ = 11 Hz, 1′, 1″), 136.8 (d, $^2J_{CP}$ = 14 Hz, 6), 138.6 (d, $^1J_{CP}$ = 14 Hz, 1), 167.4 (7), 172.9 (A1). ^{31}P NMR ($CDCl_3$, 242.93 MHz) δ/ppm: −5.13. ESI-MS (*m*/*z*): 903.3 (M + H$^+$, 100%). MALDI-HRMS (*m*/*z*): calcd 903.3223 ($C_{56}H_{48}N_4O_4P_2$ + H$^+$), found 903.3233.

9A$_p$. 4-(Diphenylphosphino)benzoic acid (145.4 mg, 0.48 mmol), HOBt (67.4 mg, 0.50 mmol), TBTU (151.3 mg, 0.47 mmol), DIPEA (0.235 mL, 1.42 mmol), **Boc-9A** (125.8 mg, 0.24 mmol), DCM (50 mL). Chromatography (EtOAc/hexane gradient; TLC, R_f = 0.21, EtOAc/hexane 1/1). Yield: 105.3 mg (49%). ^{1}H NMR ($CDCl_3$, 600.14 MHz) δ/ppm: 1.52 (d, 6H, *J* = 7 Hz), 4.04 (dd, 2H, J_1 = 17.5 Hz, J_2 = 4.5 Hz), 4.33 (dd, 2H, J_1 = 17.5 Hz, J_2 = 6.5 Hz), 4.90−4.95 (m, 2H), 7.18−7.22 (m, 6H), 7.25−7.27 (m, 8H), 7.29−7.33 (m, 14H), 7.49 (d, 2H, *J* = 8 Hz), 7.62 (dd, 2H, J_1 = 6 Hz, J_2 = 4.5 Hz), 7.72 (dd, 2H, J_1 = 8 Hz, J_2 = 1 Hz). ^{13}C NMR ($CDCl_3$, 75.48 MHz) δ/ppm: 18.2 (β), 30.3 (a), 49.2 (α), 81.6 (b), 88.9 (c), 125.9 (d), 127.3 (d, $^3J_{CP}$ = 6.5 Hz, 3,5), 128.2 (f), 128.8 (d, $^3J_{CP}$ = 7 Hz, 3′, 3″), 129.2 (4′, 4″), 131.7 (e), 133.5 (d, $^2J_{CP}$ = 19 Hz, 2,6), 133.7 (4), 134.0 (d, $^2J_{CP}$ = 20 Hz, 2′, 2″), 136.4, 136.4 (d, $^1J_{CP}$ = 11 Hz, 1′, 1″), 142.6 (d, $^1J_{CP}$ = 14 Hz, 1), 167.5 (7), 173.0 (A1). ESI-MS (*m*/*z*): 941.3 (M + K$^+$, 5%). MALDI-HRMS (*m*/*z*): calcd 925.3043 ($C_{56}H_{48}N_4O_4P_2$ + H$^+$), found 925.3026.

9V. 3-(Diphenylphosphino)benzoic acid (114.1 mg, 0.37 mmol), HOBt (49.7 mg, 0.37 mmol), TBTU (119.6 mg, 0.37 mmol), DIPEA (0.130 mL, 0.79 mmol), **Boc-9V** (110.0 mg, 0.19 mmol), DCM (50 mL). Chromatography (EtOAc/hexane gradient; TLC, R_f = 0.41, EtOAc/hexane 1/1). Yield: 84.8 mg (47%). ^{1}H NMR ($CDCl_3$, 300.14 MHz) δ/ppm: 0.97 (d, 6H, *J* = 6.5 Hz), 0.98 (d, 6H, *J* = 6.5 Hz), 2.15−2.27 (m, 2H), 3.95 (dd, 2H, J_1 = 17.5 Hz, J_2 = 4.5 Hz), 4.35 (dd, 2H, J_1 = 17.5 Hz, J_2 = 6.5 Hz), 4.60 (dd, 2H, J_1 = J_2 = 8.5 Hz), 7.17−7.35 (m, 30H), 7.71−7.78 (m, 6H). ^{13}C NMR ($CDCl_3$, 75.48 MHz) δ/ppm: 19.0, 19.5 (γ), 30.0 (a), 31.0 (β), 59.5 (α), 81.3 (b), 89.0 (c), 125.8 (d), 127.6 (4), 128.0 (f), 128.7 (5, under the 3′ peak), 128.7 (d, $^3J_{CP}$ = 7 Hz, 3′, 3″), 129.1 (4′, 4″), 131.8 (e), 132.9 (d, $^2J_{CP}$ = 24 Hz, 2), 133.9 (d, $^2J_{CP}$ = 20 Hz, 2′), 133.9 (d, $^2J_{CP}$ = 20 Hz, 2″), 134.2 (d, $^3J_{CP}$ = 7 Hz, 3), 136.6 (d, $^1J_{CP}$ = 10.5 Hz, 1′), 136.6 (d, $^1J_{CP}$ = 10.5 Hz, 1″), 136.8 (d, $^2J_{CP}$ = 16 Hz, 6), 138.5 (d, $^1J_{CP}$ = 13 Hz, 1), 167.6 (7), 172.0 (V1). ESI-MS (*m*/*z*): 981.4 (M + Na$^+$, 22%). MALDI-HRMS (*m*/*z*): calcd 959.3849 ($C_{60}H_{56}N_4O_4P_2$ + H$^+$), found 959.3851.

9L. 3-(Diphenylphosphino)benzoic acid (90.3 mg, 0.30 mmol), HOBt (40.4 mg, 0.30 mmol), TBTU (93.0 mg, 0.29 mmol), DIPEA (0.100 mL, 0.61 mmol), **Boc-9L** (83.7 mg, 0.14 mmol), DCM (50 mL). Chromatography (EtOAc/hexane gradient; TLC, R_f = 0.28, EtOAc/hexane 1/1). Yield: 51.1 mg (38%). ^{1}H NMR ($CDCl_3$, 600.14 MHz) δ/ppm: 0.88 (d, 6H, *J* = 6 Hz), 0.90 (d, 6H, *J* = 6 Hz), 1.62−1.76 (m, 6H), 3.85 (dd, 2H, J_1 = 17.5 Hz, J_2 = 4.5 Hz), 4.27 (dd, 2H, J_1 = 17.5 Hz, J_2 = 6.5 Hz), 4.83−4.87 (m, 2H), 7.11 (d, 2H, *J* = 8 Hz), 7.17−7.19 (m, 2H), 7.22 (t, 2H, *J* = 7.5 Hz), 7.25−7.34 (m, 20H), 7.69 (d, 2H, *J* = 8 Hz), 7.76 (d, 2H, *J* = 8 Hz), 7.79 (pseudo-t, 2H, *J* = 5.5 Hz). ^{13}C NMR ($CDCl_3$, 75.48 MHz) δ/ppm: 22.2, 23.1 (δ), 25.0 (γ), 30.1 (a), 41.0 (β), 52.3 (α), 81.3 (b), 89.0 (c), 125.6 (d), 127.5 (4), 127.9 (f), 128.7 (d, $^3J_{CP}$ = 7 Hz, 3′, 3″), 128.8 (5, under the 3′ peak), 129.1, 129.1 (4′, 4″), 131.8 (e), 132.8 (d, $^2J_{CP}$ = 23 Hz, 2), 133.9 (d, $^2J_{CP}$ = 19.5 Hz, 2′), 133.9 (d, $^2J_{CP}$ = 19.5 Hz, 2″), 134.0 (d, $^3J_{CP}$ = 7 Hz, 3), 136.6 (d, $^1J_{CP}$ = 11 Hz, 1′), 136.6 (d, $^1J_{CP}$ = 11 Hz, 1″), 136.8 (d, $^2J_{CP}$ = 16.5 Hz, 6), 138.4 (d, $^1J_{CP}$ = 13 Hz, 1), 167.5 (7), 172.9 (L1). ESI-MS (*m*/*z*): 1009.4 (M + Na$^+$, 29%). MALDI-HRMS (*m*/*z*): calcd 987.4162 ($C_{62}H_{60}N_4O_4P_2$ + H$^+$), found 987.4164.

9L$_p$. 4-(Diphenylphosphino)benzoic acid (80.4 mg, 0.26 mmol), HOBt (37.5 mg, 0.28 mmol), TBTU (85.4 mg, 0.27 mmol), DIPEA (0.090 mL, 0.55 mmol), **Boc-9L** (75.9 mg, 0.12 mmol), DCM (50 mL). Chromatography (EtOAc/hexane gradient; TLC, R_f = 0.33, EtOAc/hexane 1/1). Yield: 36.7 mg (30%). ^{1}H NMR ($CDCl_3$, 600.14 MHz) δ/ppm: 0.93 (d, 6H, *J* = 6 Hz), 0.95 (d, 6H, *J* = 6 Hz), 1.52−1.56 (m, 2H), 1.71−1.78 (m, 4H), 3.92 (dd, 2H, J_1 = 17.5 Hz, J_2 = 4 Hz), 4.30 (dd, 2H, J_1 = 17.5 Hz, J_2 = 7 Hz), 4.86−4.90 (m, 2H), 7.25−7.20 (m, 8H), 7.26−7.35 (m, 26H), 7.66−7.67 (m, 6H). ^{13}C NMR (DMSO-d_6, 75.48 MHz) δ/ppm: 21.2, 23.0 (δ), 24.4 (γ), 28.9 (a), 40.3 (β), 51.7 (α), 80.0 (b), 90.9 (c), 124.8 (d), 127.7 (d, $^3J_{CP}$ = 7 Hz, 3, 5), 128.4 (f), 128.8 (d, $^3J_{CP}$ = 7 Hz, 3′, 3″), 129.2 (4′, 4″), 131.8 (e), 132.7 (d, $^2J_{CP}$ = 19 Hz, 2), 133.3 (d, $^2J_{CP}$ = 20 Hz, 2′, 2″), 134.3 (4), 136.0 (d, $^1J_{CP}$ = 11 Hz, 1′), 136.1 (d, $^1J_{CP}$ = 11 Hz, 1″), 140.7 (d, $^1J_{CP}$

dx.doi.org/10.1021/om5005385 | *Organometallics* 2014, 33, 4005−4015

= 13 Hz, 1), 166.0 (7), 172.1 (L1). ESI-MS (m/z): 1009.4 ($M + Na^+$, 18%). MALDI-HRMS (m/z): calcd 1009.3982 ($C_{62}H_{60}N_4O_4P_2 + Na^+$), found 1009.3978.

9F. 3-(Diphenylphosphino)benzoic acid (98.6 mg, 0.32 mmol), HOBt (47.5 mg, 0.35 mmol), TBTU (103.7 mg, 0.32 mmol), DIPEA (0.200 mL, 1.21 mmol), **Boc-9F** (101.6 mg, 0.15 mmol), DCM (50 mL). Chromatography (EtOAc/hexane gradient; TLC, R_f = 0.47, EtOAc/hexane 1/1). Yield: 69.7 mg (44%). ^{1}H NMR ($CDCl_3$, 600.14 MHz) δ/ppm: 3.11 (dd, 2H, J_1 = 14 Hz, J_2 = 8 Hz), 3.20 (dd, 2H, J_1 = 14 Hz, J_2 = 7 Hz), 3.90 (dd, 2H, J_1 = 17.5 Hz, J_2 = 4.5 Hz), 4.20 (dd, 2H, J_1 = 17.5 Hz, J_2 = 6 Hz), 5.02−5.06 (m, 2H), 7.09−7.33 (m, 40H), 7.49 (t, 2H, J = 5.5 Hz), 7.61 (d, 2H, J = 7.5 Hz), 7.72 (d, 2H, J = 8 Hz). ^{13}C NMR ($CDCl_3$, 75.48 MHz) δ/ppm: 30.1 (a), 38.5 (β), 55.1 (α), 81.5 (b), 88.8 (c), 125.7 (d), 127.0 (ζ), 127.6 (4), 128.1 (f), 128.6 (δ), 128.7 (5, under the 3′ peak), 128.8 (d, $^3J_{CP}$ = 7 Hz, 3′, 3″), 129.1 (4′, 4″), 129.4 (ε), 131.8 (e), 132.8 (d, $^2J_{CP}$ = 24 Hz, 2), 133.9 (d, $^2J_{CP}$ = 20 Hz, 2′, 2″), 133.9 (d, $^3J_{CP}$ = 7.5 Hz, 3), 136.6 (d, $^1J_{CP}$ = 11 Hz, 1′), 136.6 (d, $^1J_{CP}$ = 11 Hz, 1″), 136.8 (γ), 136.8 (d, $^2J_{CP}$ = 15.5 Hz, 6), 138.5 (d, $^1J_{CP}$ = 13.5 Hz, 1), 167.5 (7), 171.7 (F1). ESI-MS (m/z): 1055.2 ($M + H^+$, 39%). MALDI-HRMS (m/z): calcd 1055.3849 ($C_{68}H_{56}N_4O_4P_2 + H^+$), found 1055.3872.

10A. 3-(Diphenylphosphino)benzoic acid (66.4 mg, 0.22 mmol), HOBt (29.4 mg, 0.22 mmol), TBTU (69.6 mg, 0.22 mmol), DIPEA (0.145 mL, 0.88 mmol), **Boc-10A** (100.0 mg, 0.19 mmol), DCM (50 mL). Chromatography (EtOAc/hexane gradient; TLC, R_f = 0.21, EtOAc/hexane 7/3). Yield: 26.6 mg (27%). ^{1}H NMR (DMSO-d_6, 300.13 MHz) δ/ppm: 1.31 (d, 6H, J = 7 Hz), 1.57−1.67 (m, 4H), 2.52−2.56 (m, 4H, solvent overlapped), 3.03−3.15 (m, 4H), 4.36−4.46 (m, 2H), 7.05−7.13 (m, 4H), 7.22−7.31 (m, 10H), 7.38−7.42 (m, 11H), 7.45−7.51 (m, 3H), 7.89−7.95 (m, 6H), 8.54 (d, 2H, J_1 = 7.5 Hz, J_2 = 1 Hz). ^{13}C NMR (DMSO-d_6, 75.48 MHz) δ/ppm: 18.0 (β), 29.1 (c), 30.7 (b), 38.4 (a), 49.1 (α), 125.8 (f), 128.0 (4), 128.6 (d, $^3J_{CP}$ = 6 Hz, 5), 128.8 (d, $^3J_{CP}$ = 7 Hz, 3′, 3″), 128.9 (e), 129.1, (4′, 4″), 132.7 (d, $^2J_{CP}$ = 26 Hz, 2), 133.2 (d, $^2J_{CP}$ = 20 Hz, 2′), 133.2 (d, $^2J_{CP}$ = 20 Hz, 2″), 134.3 (d, $^3J_{CP}$ = 8 Hz, 3), 135.6 (d, $^2J_{CP}$ = 14 Hz, 6), 136.2 (d, $^1J_{CP}$ = 11 Hz, 1′), 136.2 (d, $^1J_{CP}$ = 11 Hz, 1″), 137.0 (d, $^1J_{CP}$ = 12.5 Hz, 1), 139.4 (d), 165.5 (7), 172.1 (A1). ESI-MS (m/z): 911.4 ($M + H^+$, 34%). MALDI-HRMS (m/z): calcd 911.3849 ($C_{56}H_{56}N_4O_4P_2 + H^+$), found 911.3828.

10A$_p$. 4-(Diphenylphosphino)benzoic acid (66.0 mg, 0.22 mmol), HOBt (67.4 mg, 0.50 mmol), TBTU (70.0 mg, 0.22 mmol), DIPEA (0.145 mL, 0.88 mmol), **Boc-10A** (100.0 mg, 0.19 mmol), DCM (50 mL). Chromatography (EtOAc/hexane gradient; TLC, R_f = 0.24, EtOAc/hexane 7/1). Yield: 58.2 mg (59%). ^{1}H NMR (DMSO-d_6, 300.13 MHz) δ/ppm: 1.32 (d, 6H, J = 7 Hz), 1.59−1.69 (m, 4H), 2.52−2.57 (m, 4H), 3.07−3.15 (m, 4H), 4.39−4.48 (m, 2H), 7.05−7.13 (m, 4H), 7.23−7.31 (m, 12H), 7.39−7.43 (m, 12H), 7.88 (dd, 4H, J_1 = 8 Hz, J_2 = 1 Hz), 7.94 (pseudo-t, 2H, J = 5.5 Hz), 8.46 (d, 2H, J = 7.5 Hz). ^{13}C NMR (DMSO-d_6, 75.48 MHz) δ/ppm: 18.0 (β), 29.2 (c), 30.7 (b), 38.4 (a), 49.1 (α), 125.8 (f), 127.7 (d, $^3J_{CP}$ = 6.5 Hz, 3,5), 128.8 (d, $^3J_{CP}$ = 7 Hz, 3′, 3″), 128.9 (e), 129.2 (4′, 4″), 132.7 (d, $^2J_{CP}$ = 19 Hz, 2), 133.3 (d, $^2J_{CP}$ = 19.5 Hz, 2′, 2″), 133.4 (4), 136.1 (d, $^1J_{CP}$ = 11 Hz, 1′, 1″), 139.4 (d), 140.65 (d, $^1J_{CP}$ = 13.5 Hz, 1), 165.6 (7), 172.1 (A1). ESI-MS (m/z): 925.4 ($M + H^+$, 32%). MALDI-HRMS (m/z): calcd 925.3043 ($C_{56}H_{48}N_4O_4P_2 + Na^+$), found 925.3026.

10L. 3-(Diphenylphosphino)benzoic acid (109.2 mg, 0.36 mmol), HOBt (50.7 mg, 0.38 mmol), TBTU (113.4 mg, 0.35 mmol), DIPEA (0.120 mL, 0.73 mmol), **Boc-10L** (105.0 mg, 0.17 mmol), DCM (50 mL). Chromatography (EtOAc/hexane gradient; TLC, R_f = 0.47, EtOAc/hexane 1/1). Yield: 57.8 mg (33%). ^{1}H NMR ($CDCl_3$, 600.14 MHz) δ/ppm: 0.89 (d, 6H, J = 6.5 Hz), 0.90 (d, 6H, J = 6.5 Hz), 1.42−1.57 (m, 4H), 1.61−1.70 (m, 6H), 2.28−2.33 (m, 2H), 2.42−2.47 (m, 2H), 2.66−2.70 (m, 2H), 3.48−3.54 (m, 2H), 4.86−4.90 (m, 2H), 6.86 (d, 2H, J = 9 Hz), 6.97−7.00 (m, 2H), 7.04−7.07 (m, 2H), 7.25−7.34 (m, 22H), 7.39−7.41 (m, 2H), 7.67−7.69 (m, 2H), 7.71−7.73 (m, 2H), 7.97−7.98 (m, 2H). ^{13}C NMR ($CDCl_3$, 75.48 MHz) δ/ppm: 22.4, 22.9 (δ), 25.0 (γ), 29.5 (c), 31.4 (b), 39.1 (a), 41.4 (β), 52.6 (α), 126.1 (f), 127.2 (4), 128.8 (d, $^3J_{CP}$ = 7 Hz, 3′, 3″), 128.8 (d, $^2J_{CP}$ = 6 Hz, 5), 129.2, 129.2 (4′, 4″), 129.3 (e), 132.6 (d, $^2J_{CP}$ = 21 Hz, 2), 133.8 (d, $^2J_{CP}$ = 20 Hz, 2′), 134.0 (d, $^2J_{CP}$ = 20 Hz, 2″), ≈ 133.9 (3, not observable because overlap), 136.5 (d, $^1J_{CP}$ = 11 Hz, 1′), 136.5 (d, $^1J_{CP}$ = 11 Hz, 1″), 136.9 (d, $^2J_{CP}$ = 18 Hz, 6), 138.7 (d, $^1J_{CP}$ = 13.5 Hz, 1), 139.8 (d), 167.3 (7), 172.8 (A1). ^{31}P NMR ($CDCl_3$, 242.93 MHz) δ/ppm: −4.96. ESI-MS (m/z): 1033.5 ($M + K^+$, 23%). MALDI-HRMS (m/z): calcd 1033.4374 ($C_{62}H_{68}N_4O_4P_2 + K^+$), found 1033.4388.

10L$_p$. 4-(Diphenylphosphino)benzoic acid (110.1 mg, 0.36 mmol), HOBt (49.8 mg, 0.37 mmol), TBTU (114.2 mg, 0.36 mmol), DIPEA (0.120 mL, 0.73 mmol), **Boc-10L** (105.0 mg, 0.17 mmol), DCM (50 mL). Chromatography (EtOAc/hexane gradient; TLC, R_f = 0.47, EtOAc/hexane 1/1). Yield: 63.5 mg (36%). ^{1}H NMR ($CDCl_3$, 600.14 MHz) δ/ppm: 0.94 (d, 6H, J = 6 Hz), 0.95 (d, 6H, J = 6.5 Hz), 1.49−1.60 (m, 4H), 1.67−1.77 (m, 6H), 2.35−2.46 (m, 4H), 2.85−2.90 (m, 2H), 3.48−3.54 (m, 2H), 4.90−4.93 (m, 2H), 6.98−7.00 (m, 2H), 7.03−7.05 (m, 2H), 7.20 (d, 2H, J = 9 Hz), 7.23−7.35 (m, 24H), 7.68 (dd, 2H, J_1 = 8.5 Hz, J_2 = 1 Hz), 7.84 (dd, 2H, J_1 = 8 Hz, J_2 = 4 Hz). ^{13}C NMR ($CDCl_3$, 75.48 MHz) δ/ppm: 22.4, 23.0 (δ), 25.1 (γ),29.7 (c), 31.1 (b), 39.3 (a), 41.3 (β), 52.5 (α), 81.6 (b), 88.9 (c), 126.2 (f), 127.2 (d, $^3J_{CP}$ = 6.5 Hz, 3,5), 128.8 (d, $^3J_{CP}$ = 7 Hz, 3′, 3″), 129.1 (e), 129.2 (4′, 4″), 133.5 (d, $^2J_{CP}$ = 19 Hz, 2), 133.8 (4), 134.0 (d, $^2J_{CP}$ = 20 Hz, 2′, 2″), 136.4 (d, $^1J_{CP}$ = 11 Hz, 1′, 1″), 139.6 (d), 142.7 (d, $^1J_{CP}$ = 14 Hz, 1), 167.5 (7), 172.9 (A1). ESI-MS (m/z): 1033.4 ($M + K^+$, 10%). MALDI-HRMS (m/z): calcd 1017.4608 ($C_{62}H_{68}N_4O_4P_2 + Na^+$), found 1017.4615.

Precatalytic Rh(I) Complexes. *NMR Measurements.* [Rh(COD)$(CH_3CN)_2$]BF_4 (1 mg, 2.6 μmol, 1 equiv) and ligand (2 equiv) were each dissolved in $CDCl_3$ (300 μL). Rhodium solution was added to the ligand solution, and NMR spectra were recorded shortly thereafter.

CD Measurements. Visible region (c = 0.15−0.44 mmol dm^{-3}): [Rh(COD)$(CH_3CN)_2$]BF_4 (1 equiv) and the ligand (2 equiv) were each dissolved in 2 mL of distilled, degassed CH_2Cl_2. These solutions were then mixed, and the mixture was diluted to 5.0 mL. UV region (c = 0.01−0.03 mmol dm^{-3}): 300 μL of the solution for visible measurements was diluted to 5.0 mL.

Catalysis. *Catalytic Hydrogenation of Methyl 2-Acetamidoacrylate (**S1**). Catalysis at Room Temperature.* An oven-dried, two-necked, round-bottomed flask (10 mL) under nitrogen was charged with the ligand (6.6 μmol, 2.2 mol %) dissolved in CH_2Cl_2 (3 mL; distilled, degassed in an ultrasonic bath for 15 min), followed by [Rh(COD)$(CH_3CN)_2$]BF_4 (1.25 mg, 3 μmol, 1 mol %) dissolved in CH_2Cl_2 (2 mL). Several experiments were performed in diluted CH_2Cl_2 solution (total volume 50 mL instead of 5 mL) or in methanol (total volume 5 mL). The flask was then flushed with hydrogen, and **S1** (45 mg, 0.3 mmol) was added in one portion and the mixture vigorously stirred with a magnetic stirrer. After 2 h, 0.5 mL of the solution was eluted through silica (150 mg) with ethyl acetate (5 mL), and the enantiomeric excess (ee) was determined with a chiral fused silica capillary column (Beta Dex 225; isocratic 140 or 150 °C; 100 kPa head column pressure; eluting order substrate, *R* product, *S* product).

Catalysis at Low Temperature. According to the procedure for reactions at room temperature before substrate addition, the reaction flask was placed in a thermo-container filled with technical ethanol (or 2-propanol), cooled by a cryostat device to −5 °C, and the mixture was stirred vigorously overnight.

*Catalytic Hydrogenation of Methyl (Z)-α-Acetamidocinnamate (**S2**). Catalysis at Atmospheric Pressure.* The procedure described for **S1** was used with ligand (13.2 μmol, 2.2 mol %), [Rh(COD)$(CH_3CN)_2$]BF_4 (2.50 mg, 6 μmol, 1 mol %), and **S2** (70 mg, 0.3 mmol). Chiral fused silica capillary column (L-Chirasil-Val; conditions 22 min at 170 °C, 40 °C min^{-1} to 190 °C, 60 kPa head column pressure; t_R = 18.30 (*R*), 18.75 (*S*), 32.39 (substrate) min).

Catalysis at High Pressure. In an Eppendorf vial, Rh precursor and the ligand were dissolved in CH_2Cl_2 (0.5 mL each) and mixed. The yellow solution was placed in a 10 mL beaker containing the substrate and CH_2Cl_2 (4 mL). The beaker was tightly sealed in an autoclave and purged three times with H_2 (13 bar) and finally stirred at 13 bar for 2 h. The product was analyzed as detailed above.

dx.doi.org/10.1021/om5005385 | *Organometallics* 2014, 33, 4005−4015

■ ASSOCIATED CONTENT

Supporting Information

Text, a table, figures, and xyz files giving synthetic procedures for the precursors **Boc-2**−**Boc-10**, catalytic asymmetric hydrogenation using para-substituted ligands, NMR and CD spectra, GC chromatograms, visualized calculated structures of various conformers and stereochemical analysis, and Cartesian coordinates for all computed molecules collected in a single separate text file readable by the program Mercury (version 3.3 or later)[33] for visualization and analysis. This material is available free of charge via the Internet at http://pubs.acs.org.

■ AUTHOR INFORMATION

Corresponding Author

*E-mail for S.I.K.: Srecko.Kirin@irb.hr.

Notes

The authors declare no competing financial interest.

■ ACKNOWLEDGMENTS

These materials are based on work financed by the Unity Through Knowledge Fund (UKF, 36/08), the Croatian Science Foundation (HrZZ, 02.04/23), and the Ministry of Science, Education and Sports (MSES, 098-0982904-2946, 098-0982933-2908 and 098-0982933-2936). We thank COST Action CM1105 for financial support.

■ REFERENCES

(1) Liskamp, R. M. J.; Rijkers, D. T. S.; Kruijtzer, J. A. W.; Kemmink, J. *ChemBioChem* **2011**, *12*, 1626−1653.

(2) (a) Vasudev, P. G.; Chatterjee, S.; Shamala, N.; Balaram, P. *Chem. Rev.* **2011**, *111*, 657−687. (b) Vagner, J.; Qu, H.; Hruby, V. J. *Curr. Opin. Chem. Biol.* **2008**, *12*, 292−296.

(3) Kahn, M.; Eguchi, M. In *Synthesis of peptides and peptidomimetics*, 4th ed.; Goodman, M., Felix, A. F., Moroder, L., Toniolo, C., Eds.; Georg Thieme Verlag: Stuttgart, Germany, 2004; Vol. *E22c*, pp 695−758.

(4) Chouhan, G.; James, K. *Org. Lett.* **2013**, *15*, 1206−1209.

(5) Hack, V.; Reuter, C.; Opitz, R.; Schmieder, P.; Beyermann, M.; Neudorfl, J.-M.; Kuhne, R.; Schmalz, H.-G. *Angew. Chem., Int. Ed.* **2013**, *52*, 1−6.

(6) Garland, S. L.; Dean, P. M. *J. Comput.-Aided Mol. Des.* **1999**, *13*, 469−483.

(7) Grdičak, M.; Bregović, N.; Carić, D.; Jerić, I. *J. Inorg. Biochem.* **2012**, *116*, 45−52.

(8) (a) Kokan, Z.; Kirin, S. I. *Eur. J. Org. Chem.* **2013**, 8154−8161. (b) Kokan, Z.; Kirin, S. I. *RSC Adv.* **2012**, *2*, 5729−5737.

(9) Other catalysts with prochiral metal coordination spheres: (a) Kanda, K.; Oshima, S.; Shizuno, T.; Hamanaka, R.; Fukai, M.; Shibata, T. *Heterocycles* **2014**, *88*, 1355−1370. (b) Raynal, M.; Portier, F.; van Leeuwen, P. W. N. M.; Bouteiller, L. *J. Am. Chem. Soc.* **2013**, *135*, 17687−17690. (c) van Leeuwen, P. W. N. M.; Rivillo, D.; Raynal, M.; Freixa, Z. *J. Am. Chem. Soc.* **2011**, *133*, 18562−18565. (d) Laungani, A. C.; Breit, B. *Chem. Commun.* **2008**, 844−846.

(10) Other hydrogenation catalysts: (a) Wang, X.-B.; Goto, M.; Han, L.-B. *Chem. Eur. J.* **2014**, *20*, 3631−3635. (b) Thacker, N. C.; Moteki, S. A.; Takacs, J. M. *ACS Catal.* **2012**, *2*, 2743−2752. (c) Pignataro, L.; Boghi, M.; Civera, M.; Carboni, S.; Piarulli, U.; Gennari, C. *Chem. Eur. J.* **2012**, *18*, 1383−1400. (d) Dydio, P.; Rubay, C.; Gadzikwa, T.; Lutz, M.; Reek, J. N. H. *J. Am. Chem. Soc.* **2011**, *133*, 17176−17179. (e) Sambasivan, R.; Ball, Z. T. *J. Am. Chem. Soc.* **2010**, *132*, 9289−9291. (f) Gilbertson, S. R.; Collibee, S. E.; Agarkov, A. *J. Am. Chem. Soc.* **2000**, *122*, 6522−6523.

(11) Recent reviews on bioinspired catalysis: (a) Raynal, M.; Ballester, P.; Vidal-Ferran, A.; van Leeuwen, P. W. N. M. *Chem. Soc. Rev.* **2014**, *43*, 1660−1733. (b) Lewis, J. C. *ACS Catal.* **2013**, *3*, 2954−2975. (c) Dong, Z.; Luo, Q.; Liu, J. *Chem. Soc. Rev.* **2012**, *41*, 7890−7908. (d) Deuss, P. J.; Heeten, R.; Laan, W.; Kamer, P. C. J. *Chem. Eur. J.* **2011**, *17*, 4680−4698.

(12) (a) Gridnev, I. D.; Imamoto, T. *Acc. Chem. Res.* **2004**, *37*, 633−644. (b) Tangand, W.; Zhang, X. *Chem. Rev.* **2003**, *103*, 3029−3069. (c) Landis, C. R.; Halpern, J. *J. Am. Chem. Soc.* **1987**, *109*, 1746−1754. (d) Imamoto, T.; Tamura, K.; Zhang, Z.; Horiuchi, Y.; Masashi Sugiya, M.; Kazuhiro Yoshida, K.; Akira Yanagisawa, A.; Gridnev, I. D. *J. Am. Chem. Soc.* **2012**, *134*, 1754−1769.

(13) Kirin, S. I.; Kraatz, H.-B.; Metzler-Nolte, N. *Chem. Soc. Rev.* **2006**, *35*, 348−354.

(14) (a) Jarvis, A. G.; Sehnal, P. E.; Bajwa, S. E.; Whitwood, A. C.; Zhang, X.; Cheung, M. S.; Lin, Z.; Fairlamb, I. J. S. *Chem. Eur. J.* **2013**, *19*, 6034−6043. (b) Dydio, P.; Dzik, W. I.; Lutz, M.; de Bruin, B.; Reek, J. N. H. *Angew. Chem., Int. Ed.* **2011**, *50*, 396−400. (c) van Leeuwen, P. W. N. M.; Kamer, P. C. J.; Reek, J. N. H.; Dierkes, P. *Chem. Rev.* **2000**, *100*, 2741−2769.

(15) Herd, O.; Heßler, A.; Hingst, M.; Tepper, M.; Stelzer, O. *J. Organomet. Chem.* **1996**, *522*, 69−76.

(16) Grdičak, M.; Kolonić, A.; Jerić, I. *Amino Acids* **2008**, *35*, 185−194.

(17) (a) Martinez, C. R.; Iverson, B. L. *Chem. Sci.* **2012**, *3*, 2191−2201. (b) Lee, E. C.; Kim, D.; Jurecka, P.; Tarakeshwar, P.; Hobza, P.; Kim, K. S. *J. Phys. Chem. A* **2007**, *111*, 3446−3457. (c) Meyer, E. A.; Castellano, R. K.; Diederich, F. *Angew. Chem., Int. Ed.* **2003**, *42*, 1210−1250. (d) Janiak, C. *J. Chem. Soc., Dalton Trans.* **2000**, 3885−3896.

(18) For CD spectra of $[Rh(COD)(PPh_3)_2]$ derivatives see ref 8 and: Yu, J.; Rajan Babu, T. V.; Parquette, J. R. *J. Am. Chem. Soc.* **2008**, *130*, 7845−7847.

(19) For CD spectra of ferrocene peptides $[Fe(C_5H_4CO\text{-}Aa_n\text{-}R)_2]$ (Herrick conformation) see ref 13 and: Kirin, S. I.; Schatzschneider, U.; Koster, S. D.; Siebler, D.; Metzler-Nolte, N. *Inorg. Chim. Acta* **2009**, *362*, 894−906.

(20) The correlation between the CD spectra and molecular conformation is known to be rather difficult; see for example: Brkljača, Z.; Čondić-Jurkić, K.; Smith, A.-S.; Smith, D. M. *J. Chem. Theory Comput.* **2012**, *8*, 1694−1705 and references cited therein.

(21) (a) Kretschmer, R.; Schlangen, M.; Schwarz, H. *Dalton Trans.* **2013**, *42*, 4153−4162. (b) Armelin, M.; Schlangen, M.; Schwarz, H. *Chem. Eur. J.* **2008**, *14*, 5229−5236.

(22) Zhao, Y.; Truhlar, D. G. *Theor. Chem. Acc.* **2008**, *120*, 215−241.

(23) (a) Leseurre, L.; d' Herouville, F. L. B.; Püntener, K.; Scalone, M.; Genet, J.-P.; Michelet, V. *Org. Lett.* **2011**, *13*, 3250−3253. (b) Preetz, A.; Drexler, H.-J.; Schulz, S.; Heller, D. *Tetrahedron: Asymmetry* **2010**, *21*, 1226−1231. (c) Kaganovsky, L.; Cho, K.-B.; Gelman, D. *Organometallics* **2008**, *27*, 5139−5145. (d) Punniyamurthy, T.; Mayr, M.; Dorofeev, A. S.; Bataille, C. J. R.; Gosiewska, S.; Nguyen, B.; Cowley, A. R.; Brown, J. M. *Chem.Commun.* **2008**, 5092−5094. (e) Albers, J.; Dinjus, E.; Pitter, S.; Walter, O. *J. Mol. Catal. A: Chem.* **2004**, *219*, 41−46. (f) Nishihara, Y.; Nara, K.; Nishide, Y.; Osakada, K. *Dalton Trans.* **2004**, 1366−1375. (g) Zhang, X.; Mashima, K.; Koyano, K.; Sayo, N.; Kumobayashi, H.; Akutagawa, S.; Takaya, H. *J. Chem. Soc., Perkin Trans. 1* **1994**, 2309−2322.

(24) Bernstein, J.; Davis, R. E.; Shimoni, L.; Chang, H.-L. *Angew. Chem., Int. Ed. Engl.* **1995**, *34*, 1555−1573.

(25) Interestingly, in all known examples of triphenylphosphanes,[9d] ferrocenes,[12,26] and benzene-1,3,5-tricarboxylic acids[27] L-amino acids always induce a *P* helix of the central aromatic unit.

(26) For secondary structures in ferrocene amino acid bioconjugates see: (a) Barišić, L.; Čakić, M.; Mahmoud, K. A.; Liu, Y.-N.; Kraatz, H.-B.; Pritzkow, H.; Kirin, S. I.; Metzler-Nolte, N.; Rapić, V. *Chem. Eur. J.* **2006**, *12*, 4965−4980. (b) Heinze, K.; Beckmann, M. *Eur. J. Inorg. Chem.* **2005**, 3450−3457. (c) Moriuchi, T.; Nomoto, A.; Yoshida, K.; Ogawa, A.; Hirao, T. *J. Am. Chem. Soc.* **2001**, *123*, 68−75. (d) Herrick, R. S.; Jarret, R. M.; Curran, T. P.; Dragoli, D. R.; Flaherty, M. B.; Lindyberg, S. E.; Slate, R. A.; Thornton, L. C. *Tetrahedron Lett.* **1996**, *37*, 5289−5292.

(27) For secondary structures in amino acid bioconjugates of benzene-1,3,5-tricarboxylic acid see: (a) Sun, R.; Wang, S.; Xing, H.; Bai, J.; Li, Y.; Pan, Y.; You, X. *Inorg. Chem.* **2007**, *46*, 8451−8453.

(b) Bose, P. P.; Drew, M. G. B.; Das, A. K.; Banerjee, A. *Chem. Commun.* **2006**, 3196−3198.
(28) Frisch, M. J.; Trucks, G. W.; Schlegel, H. B.; Scuseria, G. E.; Robb, M. A.; Cheeseman, J. R.; Scalmani, G.; Barone, V.; Mennucci, B.; Petersson, G. A.; Nakatsuji, H.; Caricato, M.; Li, X.; Hratchian, H. P.; Izmaylov, A. F.; Bloino, J.; Zheng, G.; Sonnenberg, J. L.; Hada, M.; Ehara, M.; Toyota, K.; Fukuda, R.; Hasegawa, J.; Ishida, M.; Nakajima, T.; Honda, Y.; Kitao, O.; Nakai, H.; Vreven, T.; Montgomery, J. A., Jr.; Peralta, J. E.; Ogliaro, F.; Bearpark, M.; Heyd, J. J.; Brothers, E.; Kudin, K. N.; Staroverov, V. N.; Kobayashi, R.; Normand, J.; Raghavachari, K.; Rendell, A.; Burant, J. C.; Iyengar, S. S.; Tomasi, J.; Cossi, M.; Rega, N.; Millam, N. J.; Klene, M.; Knox, J. E.; Cross, J. B.; Bakken, V.; Adamo, C.; Jaramillo, J.; Gomperts, R.; Stratmann, R. E.; Yazyev, O.; Austin, A. J.; Cammi, R.; Pomelli, C.; Ochterski, J. W.; Martin, R. L.; Morokuma, K.; Zakrzewski, V. G.; Voth, G. A.; Salvador, P.; Dannenberg, J. J.; Dapprich, S.; Daniels, A. D.; Farkas, Ö.; Foresman, J. B.; Ortiz, J. V.; Cioslowski, J.; Fox, D. J. *Gaussian 09, Revision A.02*; Gaussian, Inc., Wallingford, CT, 2009.
(29) (a) Becke, A. D. *J. Chem. Phys.* **1993**, *98*, 5648−5652. (b) Lee, C.; Yang, W.; Parr, R. G. *Phys. Rev. B* **1988**, *37*, 785−789. (c) Miehlich, B.; Savin, A.; Stoll, H.; Preuss, H. *Chem. Phys. Lett.* **1989**, *157*, 200−206.
(30) (a) Schäfer, A.; Horn, H.; Ahlrichs, R. *J. Chem. Phys.* **1992**, *97*, 2571−2577. (b) Schäfer, A.; Huber, C.; Ahlrichs, R. *J. Chem. Phys.* **1994**, *100*, 5829−5835.
(31) (a) Hay, P. J.; Wadt, W. R. *J. Chem. Phys.* **1985**, *82*, 270−283. (b) Hay, P. J.; Wadt, W. R. *J. Chem. Phys.* **1985**, *82*, 299−310. (c) Wadt, W. R.; Hay, P. J. *J. Chem. Phys.* **1985**, *82*, 284−298.
(32) Schaftenaar, G.; Nordik, J. H. *J. Comput.-Aided Mol. Design* **2000**, *14*, 123−134.
(33) The program Mercury is available at no cost from www.ccdc.cam.ac.uk/products/mercury.